Supplementary Materials

Molecular networking assisted discovery and biosynthesis elucidation of the antimicrobial spiroketal epicospirocins

Guoliang Zhu[1,‡], Chengjian Hou[1,‡], Weize Yuan[1], Zhenzhen Wang[1], Jingyu Zhang[1], Lan Jiang[1], Loganathan Karthik[2], Bixiao Li[1], Biao Ren[3], Kangjie Lv[1], Wanying Lu[1], Zhanren Cong[1], Huanqin Dai[4], Tom Hsiang[5], Lixin Zhang[1], and Xueting Liu[1,*]

[1]*State Key Laboratory of Bioreactor Engineering, East China University of Science and Technology, Shanghai 200237, China*

[2]R and D Center, Salem microbes private Limited, Salem, Tamilnadu, India.

[3]*State Key Laboratory of Oral Diseases & National Clinical Research Center for Oral Diseases, West China Hospital of Stomatology, Sichuan University, Chengdu, 610041, China*

[4]*Chinese Academy of Sciences Key Laboratory of Pathogenic Microbiology and Immunology, Institute of Microbiology, Chinese Academy of Sciences, Beijing, 100101, China*

[5]School of Environmental Sciences, University of Guelph, Guelph, Ontario N1G 2W1, Canada

‡The authors contributed to this work equally.

*Corresponding authors. E-mail: liuxueting@ecust.edu.cn (X. Liu)

Table of contents

Supplementary Text

1. General experimental procedures

NMR spectra were acquired on a Bruker Avance DRX600 spectrometer. Chemical shifts were calibrated internally against the residual signal of the solvent in which the sample was dissolved (DMSO-d_6 δ_H 2.50 and δ_C 39.5), and all deuterated solvents were from Cambridge Isotope Laboratories (CIL). HRESIMS measurements were obtained on a Thermal Fisher Orbitrap Q Exactive mass spectrometer. ODS-A (YMC, Japan) and Sephadex LH-20 (GE Healthcare BioSciences AB) were used for purification. RP-HPLC was performed on an Agilent 1100 Series separation module with a diode array detector. Semipreparative HPLC was carried out using a Cosmosil π-nap column (10 × 250 mm, 5 μm) and YMC-pack Ph column (10 × 250 mm, 5 μm). UV-vis spectra were obtained on a Cary 50 spectrophotometer. The CD spectra was recorded on a Chirascan circular dichroism spectrometer using MeOH as solvent. Optical rotation was measured using a Perkin-Elmer Model 343 polarimeter with a 5-cm cell. Biological reagents, chemicals, and media were purchased from standard commercial sources unless stated otherwise.

2. Microbial strain culture, identification, and genome sequencing

Fungal pathogen strain EN09116 was isolated from grass, in 2011, and stored at -80°C. It was cultured on potato dextrose agar (PDA) for laboratory experiments. DNA extraction of EN09116 was carried out using CTAB (cetyltrimethylammonium bromide) as described previously[1]. Strain EN09116 was identified by morphological[2, 3] and 18S ribosomal DNA analyses. Multiple sequence alignments of 18S sequences from related species were carried out using CLUSTAL W[4]. A pair of primers (F: TCCTCCGCTTATTGATATGC (5'-3'), R: GGAAGTAAAAGTCGTAACAAGG (5'-3')) was used to amplify the 18S ribosomal DNA. A phylogenetic tree was constructed using the neighbor-joining method[5] with MEGA 7.0[6]. Bootstrap values were generated by resampling 1000 replicates. This strain has been deposited at the China General Microbiological Culture Collection Center (accession no. 19368). The nucleotide sequences of 18S rRNA gene (accession no. MN796257) and the putative secondary metabolite gene cluster (accession no. MN970214) of EN09116 have been

deposited in GenBank.

Genomic sequencing of strain EN09116 was performed at the McGill University and Génome Québec Innovation Centre (Montréal, Canada) on an Illumina HiSeq 2000 using 100-bp paired-end sequencing from Truseq DNA Libraries. Reads were assembled from the raw data with a range of Kmers (49–91) using three different programs: AbySS[7], SOAP[8], and Velvet[9]. Annotation and gene prediction of the draft genome assembly were carried out using GeneWise[10].

3. Characterization of strain EN09116.

After incubation at 28°C for 10 days, strain EN09116 formed hazel-pigmented, flocculent colonies resembling those of E. nigrum, and this identification was further confirmed by observations of vigorous aerial mycelial growth, irregular margins, intense orange colour (top view) and orange to dark red colour (reverse) in PDA medium as previously described (Fig. S8b)[11]. A phylogenetic tree (Fig. S8a) of 18S sequences revealed that EN09116 is most similar to E. nigrum CBS 231.59 (99.10%, accession number MH857847). Small scale fermentation of strain EN09116 on rice media was performed, and an EtOAc (EA) crude extract was obtained for further LC-MS/MS experiments and molecular networking analysis.

4. LC-MS/MS analysis and molecular network analysis.

Samples were analysed using a Thermal LC-MS/MS system comprised of a Thermal UltiMate 3000 UHPLC (Thermo Fisher Scientific Inc., Shanghai, China) equipped with a Waters ACQUITY BEH C18 column (150 mm × 4.6 mm, 1.7 μm particles), running an acidic water/ACN gradient, which was coupled to a Thermo Scientific Q Exactive Obitrap mass spectrometer (Thermo Fisher Scientific Inc., Shanghai, China) equipped with an ESI source operating in negative polarity. The 50 mg/L MeOH solution of EN09116 extract was analysed using an optimized data-dependent acquisition mode consisting of a full MS survey scan (70,000 resolution) in the 100–1000 Da range (scan time: 50 ms) followed by an MS/MS scan (17,500 resolution) of the 5 most intense ions in the HCD trap. The collision energy was applied at 26 eV.

The MS/MS data were converted from standard .raw (Thermal standard data-

format) to .mzML (GNPS uploading format) using MSConvert software, which is part of the ProteoWizard (vers. 3.0.4738) project. Converted data-files were processed using the molecular networking method developed by Dorrestein and co-workers[12]. The following settings were used to generate the network: minimum pairs, Cos 0.65; parent mass tolerance, 1.0 Da; ion tolerance, 0.5; network topK, 100; minimum matched peaks, 6; and minimum cluster size, 2. The molecular networking workflow is publicly available online. The molecular networking data were analysed and visualized using Cytoscape (vers. 3.7.2).

5. Fermentation, extraction, and isolation.

Strain EN09116 was cultured on PDA at 28°C for 10 days, and agar plugs (5-mm-diameter) were placed into three Erlenmeyer flasks (250 mL), each containing 100 mL of potato dextrose broth (PDB). The flasks were incubated at 28°C on a rotary shaker at 200 rpm for 5 days to generate the seed, from which 3 mL of culture was separately inoculated into 95 aseptic-bags, each containing 80 g of autoclaved rice and 120 mL distilled H_2O. These aseptic-bags were transferred to an incubator and fermented at 28°C for 35 days. Then, 7.6 kg of whole cultures were extracted with EtOAc (3 × 20 L) and concentrated under reduced pressure to yield a dark brown gum (61.7 g).

The extracts were fractionated by silica gel vacuum liquid chromatography (85 × 200-mm column) using a CH_2Cl_2-MeOH gradient (1:0, 100:1, 50:1, 20:1, 10:1, 4:1, 1:1, 0:1) to afford 10 fractions (G1–G10). G5 (14.5 g) was applied to a Sephadex LH-20 column (4 × 108-mm) using MeOH as the mobile phase to yield 23 sub-fractions (G5N1–G5N23). LC-MS analysis of these fractions revealed eight potential novel analogues of eleganketal A in G5N7 based on the characteristic UV absorption and HR-MS. Then, G5N7 (816.5 mg) was further fractionated by ODS-MPLC using gradient elution from 10% to 100% ACN-H_2O for 60 min to afford 17 sub-fractions (G5N7M1–G5N7M17). Further LC-MS guided detection located the targeted compounds in four fractions (G5N7M-10,12,15,17). G5N7M15 (114.0 mg) was purified by semi-preparative RP-HPLC using YMC-Ph (10 × 250 mm) with a flow rate of 4.0 mL/min and a gradient elution (0 min, 20% MeOH-H_2O; 20 min 50% MeOH) to obtain **1** (5.0 mg, t_R = 8.5 min) and **2** (8.0 mg, t_R = 14.5 min). G5N7M17 (136.0 mg) was purified by

semi-preparative RP-HPLC using a Cosmosil π-nap (10 × 250 mm) eluted at a flow rate of 4.0 mL/min using 30% MeOH-H_2O to obtain **3** (10.0 mg, t_R = 12.3 min) and **4** (9.0 mg, t_R = 15.7 min). G5N7M10 (12.0 mg) was purified by semi-preparative RP-HPLC using a Cosmosil π-nap (10 × 250 mm) eluted at a flow rate of 4.0 mL/min with 22% ACN-H_2O to obtain 1.9 mg of **5** (t_R = 6.5 min) and **6** (t_R = 8.2 min). G5N7M12 (60.2 mg) was purified by semi-preparative RP-HPLC using a Cosmosil π-nap (10 × 250 mm) eluted at a flow rate of 4.0 mL/min with 35% MeOH-H_2O to obtain 3.8 mg of **7** (t_R = 7.4 min) and **8** (t_R = 12.1 min).

6. Structure elucidation of compounds 1-8.

(±)-Epicospirocin A (**1a**/**1b**) was isolated as amorphous, pale yellow powder. The molecular formula $C_{19}H_{18}O_{10}$ was deduced by HRESIMS ($[M-H]^-$ at *m/z* 405.0818, calcd. for 405.0827) (Supplementary Fig. S1), indicating 11 units of unsaturation. The ^1H, ^{13}C, and HSQC NMR data (Supplementary Fig. S10-S12, S6; Table S7) of **1** revealed twelve aromatic quaternary carbons, including six oxygenated carbons, one ketone group (δ_C 192.5), one ketal group (δ_C 105.8), one *O*-methylene ($\delta_{C/H}$ 60.8/5.06&4.86) and two methyl groups ($\delta_{C/H}$ 9.9/1.96; 11.6/1.82). All of these resonances are similar to those of the marine endophytic fungi sourced polyketone eleganketal A, except for the existence of an additional acetal methine ($\delta_{C/H}$ 105.6/6.15) and methoxyl moiety ($\delta_{C/H}$ 52.7/3.24), indicating **1** is an analogue of eleganketal A. The HMBC correlations from H-10 (δ_H 3.24) to C-1 (δ_C 105.6); and H-1 (δ_H 6.15) to C-10 (δ_C 52.7), C-7 (δ_C 128.4), and C-8 (δ_C 105.8) position the -OCH_3 (C-10) at C-1. While HMBC correlations from H-9 (δ_H 1.82) to C-5 (δ_C 146.1), C-6 (δ_C 110.4), and C-7 (δ_C 128.4); and H-9′ to C-2′ (δ_C 131.3), C-3′ (δ_C 111.5), and C-4′ (δ_C 153.6) position the two methyl moieties (C-9/9′) connected at C-6 and C-3′, which was distinguished from that of eleganketal A. Further detailed analysis of the other HMBC correlations revealed **1** shared a 5,6,7-trihydroxy-8-methylisochroman-4-one fragment with eleganketal A (Supplementary Figs. S13 and S15). Thus, the planar structure of **1** was elucidated as showed in Supplementary Fig. S4. The -OCH_2 (C-1′) at C-8 and -OCH_3 (C-10) at C-1 were assigned to be in the same orientation on the 5-membered ring on the basis of key NOESY correlations from H-10 to H-1′ and H-1′ to H-9′ (Supplementary Fig. S16 and Fig. S55). Because **1** displayed no optical activity, chiral separation was carried out using HPLC with a Chiralpac IC column, resulting in a pair of enantiomers, **1a** and **1b**

(Supplementary Fig. S56). The $[\alpha]_D$ and Cotton effects in the recorded CD curves of **1a** and **1b** were completely opposite (Supplementary Figs. S57). To further establish the absolute configuration of **1a** and **1b**, the time-dependent density functional theory (TD-DFT) method was used to do an ECD calculation and simulation at the B3LYP/6-31+G(d) level. The preliminary conformational distribution search was performed by Sybyl 2.0 software. The corresponding minimum geometries were further fully optimized by using DFT at the B3LYP/6-31G(d) level as implemented in the Gaussian 03 program package (Supplementary text 7). The results showed that the measured CD curve of **1a** was well matched with the calculated ECD for 1*R*,8*R*-**1**, while the experimental CD of **1b** corresponded with the calculated ECD of 1*S*,8*S*-**1** (Supplementary Fig. S58).

(±)-1-*epi*-Epicospirocin A (**2a**/**2b**) was isolated as amorphous, pale yellow powder. The molecular formula $C_{19}H_{18}O_{10}$ was established by HRESIMS ($[M-H]^-$ at *m/z* 405.0817, calcd. for 405.0827) (Supplementary Fig. S17), with 11 units of unsaturation, equivalent to **1**. The 1D NMR of **2** was almost the same as that of **1**, except minor differences in chemical shifts on some positions in ^1H and ^{13}C NMR (Table S7; Supplementary Figs. S18-S20). The HSQC and HMBC coupling pattern of these two compounds were also highly similar, indicating they shared the same planar structure (Supplementary Fig. S55, Supplementary Figs. S21-S23). Unlike **1**, NOE coupling between H-10 and H-1′ could not be observed from the NOESY spectrum of **2**, suggesting a reversed relative configuration (Supplementary Fig. S55 and Fig. S24). Through further chiral separation and ECD calculations, the absolute configurations of enantiomers, **2a** and **2b**, were assigned as 1*S*,8*R* and 1*R*,8*S*, respectively (Supplementary Figs. S56-S58).

(±)-aspermicrone B (**3a**/**3b**) was isolated as amorphous, pale yellow powder. The molecular formula $C_{19}H_{18}O_{10}$ was established by HRESIMS ($[M-H]^-$ at *m/z* 405.0816, calcd. for 405.0827) (Supplementary Fig. S25), with 11 units of unsaturation, equivalent to **1**. The 1D NMR of **3** was highly similar to **1** (Table S7; Supplementary Figs. S26-S28), while the HMBC correlations from H-9 (δ_H 2.02) to C-2 (δ_C 128.2), C-3 (δ_C 110.3), and C-4 (δ_C 146.4); and from H-9′ to C-2′ (δ_C 131.3), C-3′ (δ_C 111.2), and C-4′ (δ_C 152.9) position the two methyls (C-9/9′) at C-3 and C-3′ (Supplementary Fig. S55 and Fig. S31). These results indicated **1** and **3** are positional isomers, and thus the planar structure of **3** is actually same as previously reported dibenzospiroketal aspermicrone

B (Supplementary Fig. S4), however unlike aspermicrone B, **3** exhibited to be racemic like **1**. The relative configuration between C-1/C-8 of **3** was same as that of **1** as deduced from the key NOESY correlations from H-10 to H-1′ and H-1′ to H-9′ (Supplementary Fig. S55 and Fig. S32). Like **1**, **3** could be further separated into a pair of enantiomers, with the absolute configurations assigned as 1*R*,8*R* for **3a** (aspermicrone B) and 1*S*,8*S* for **3b** on the basis of ECD calculations (Supplementary Fig. S56-S57, S59), **3b** was a new enantiomer of aspermicrone B, named as *ent*-aspermicrone B.

(±)-aspermicrone C (**4a**/**4b**) was isolated as amorphous, pale yellow powder. The molecular formula $C_{19}H_{18}O_{10}$ was established by HRESIMS ($[M-H]^-$ at *m/z* 405.0817, calcd. for 405.0827) (Supplementary Fig. 33), with 11 units of unsaturation, equivalent to **3**. The 1D and 2D NMR of **4** were almost the same as those of **3**, indicating they shared the same planar structure (Table S7; Supplementary Fig. S4, Fig. S42-S47). NOE coupling between H-10 and H-1′ that existed with **3** was not observed, suggesting the -OCH_2 (C-1′) at C-8 and -OCH_3 (C-10) at C-1 were on opposite sides of the 5-membered ring (Supplementary Fig. S55 and Fig. S40). The enantiomers **4a** and **4b** were obtained by chiral separation, and their absolute configurations were determined by ECD calculations to be 1*S*,8*R* (aspermicrone C) and 1*R*,8*S*, respectively (Supplementary Fig. S56-S57, S59). **4b** was a new enantiomer of aspermicrone C, named as *ent*-aspermicrone C.

The structures of epicospirocin B (**5**), 1-*epi*-epicospirocin B (**6**), epicospirocin C (**7**), 1-*epi*-epicospirocin C (**8**) were also elucidated based on the 1D&2D NMR and HRMS data (Supplementary Fig. S41-S54).

7. Theory and Calculation Details

The calculations were performed by using the density functional theory (DFT) as carried out in the Gaussian 03.[13] The preliminary conformational distributions search was performed by Sybyl-X 2.0 software. All ground-state geometries were optimized at the B3LYP/6-31G(d) level (Supplementary Fig. S60-S63). Solvent effects of methanol solution were evaluated at the same DFT level by using the SCRF/PCM method.[14] TDDFT at B3LYP/6-31+G(d) was employed to calculate the electronic excitation energies and rotational strengths in methanol (Supplementary Fig. S58-S59).[15]

8. Antimicrobial assay against *S. aureus*, MRSA, *S. mutans*, and *S. sanguis*.

Screening assays were performed in accordance with the Antimicrobial Susceptibility Testing Standards outlined by the Clinical and Laboratory Standards Institute (CLSI) and our previous report.[16] The S. aureus strain used here was an ATCC strain, ATCC6538. The methicillin-resistant S. aureus was clinically isolated by the 309th Hospital of the Chinese People's Liberation Army. The S. mutans strain used here was an ATCC strain, ATCC UA159. The S. sanguis strain used here was an ATCC strain, ATCC 10556. Bacteria from glycerol stocks were inoculated on LB agar plates and cultured overnight at 37°C. Then, single colonies were picked and adjusted to approximately 104 CFU/mL with Mueller-Hinton Broth to make a bacterial suspension. A 2-fold serial dilution series for each compound (as 2 μL in DMSO) was added to each row of a 96-well plate (F-bottom, Greiner Bio-One Ltd.) that contained 78 μL of bacteria suspension in each well. Vancomycin was used as a positive control, and DMSO was used as a negative control. The 96-well plate was aerobically incubated at 37°C for 16 h. Then, optical density values at 600 nm were measured with a Multilabel Plate Reader, yielding MIC values.

9. Antifungal Assay.

Antifungal bioassays were performed in accordance with a protocol modified from the Clinical and Laboratory Standards Institute M-27A methods[17] using the fungus Candida albicans (ATCC 5314). A colony of C. albicans was picked from a YPD agar plate and suspended in RPMI 1640 at a concentration of 1 × 104 cfu/mL. A two-fold serial dilution of each compound to be tested (4000 to 31.3 μg/mL in DMSO) was prepared, and an aliquot of each dilution (2 μL) was added to a flat-bottom, 96-well microtiter plate (Greiner). Amphotericin B was used as the positive control, and DMSO was the negative control. An aliquot (78 μL) of the fungal suspension was added to each well (to give final compound concentrations of 100 to 0.78 μg/mL in 2.5% DMSO) and the plate was incubated at 35°C for 16 h. Finally, the optical density of each well at 600 nm was measured with an EnVision 2103 Multilabel Plate Reader (Perkin-Elmer Life Sciences). Antifungal MICs were defined as the minimum concentration of

compound that inhibited visible fungal growth. All experiments were performed in triplicate.

10. Identification of NR-PKS like BGCs in EN09116 and phylogenetic analysis

Analysis of the EN09116 genome sequence was carried out using antiSMASH online software[18]. Each gene in putative NR-PKS like BGCs was analysed by BLASTP against the GenBank database[19], yielding homologous sequences. Multiple sequence alignment and evolutionary analyses were conducted in MEGA7.0[6]. From approximately 19 million sequencing reads (2 × 100 bp) and 3.8 Gb of raw data, a 35.2 Mb EN09116 genome assembly, which had the highest N50 value (Abyss Kmer 63, N50 = 392,000 bp, contigs = 6667 over 100 bp length), was built. Gene predictions yielded 9270 genes. The phylogenetic tree was inferred using the maximum likelihood method based on the Jones-Taylor-Thornton model. Bootstrap values were calculated out of 1000 replicates. All positions containing gaps or missing data were eliminated. Trees were viewed and edited using iTol[20, 21].

11. Construction of the *Δesp3* and *Δesp4* strains of EN09116

Plasmids for gene knock-out in EN09116 were constructed using the split-marker strategy. The entire *esp3* gene was deleted via homologous recombination using the deletion cassette from overlap PCR[22]. Primer pairs *esp3*-up-F/*esp3*-up-R, *esp3*-dn-F/ *esp3*-dn-R, and hph F/hph R (Table. S5) were, respectively, used to amplify *esp3* upstream and downstream homologous regions from fungal genomic DNA and the hygromycin resistance gene from plasmid pAg1-H3[23]. After agarose gel purification of DNA fragments, primers *esp3*-F and *esp3*-R were used to amplify the entire deletion cassette. The PCR product was gel purified and solubilized in STC buffer (1.2 M sorbitol, 10 mM $CaCl_2$, 10 mM Tris-HCl, pH 7.5).

Split-marker DNA was introduced into EN09116 by protoplast transformation. EN09116 mycelia were collected on PDA for 7 days at 25°C, washed twice with the osmotic medium (1.2 M $MgCl_2$, 10 mM sodium phosphate, pH 5.8), and incubated in enzyme cocktail solution (10 mg/mL lysing enzymes, 3 mg/mL yatalase in osmotic medium) at 30°C for 4 hours. After two washes with STC buffer, protoplasts were

gently mixed with DNA and incubated for 1 hour on ice. After 300 μL of PEG 4000 solution (60% PEG 4000, 50 mM $CaCl_2$, 50 mM Tris-HCl, pH 7.5) was added to 100 μL of protoplast mixture, samples were incubated at room temperature for 30 min and plated on the regeneration selection medium (RM, 0.1% Casamino acid, 0.1% Yeast extract, 27.4% sucrose, 1.6% Agar powder, 50 mg/L hygromycin B). Following incubation at 25°C for about 2 weeks, transformants were inoculated on PDA medium (with 50 mg/L hygromycin B) with stationary incubation for about 1 week to prepare the genomic DNA used to confirm genotype by PCR. Construction of the *Δesp4* strain followed a procedure similar to that used for *Δesp3*.

Supplementary Figures

Fig. S1 A overview of GNPS MS/MS molecular network generated for EA extract of EN09116 with a cosine similarity score cutoff of 0.65 (generated using Cytoscape v3.7.2)

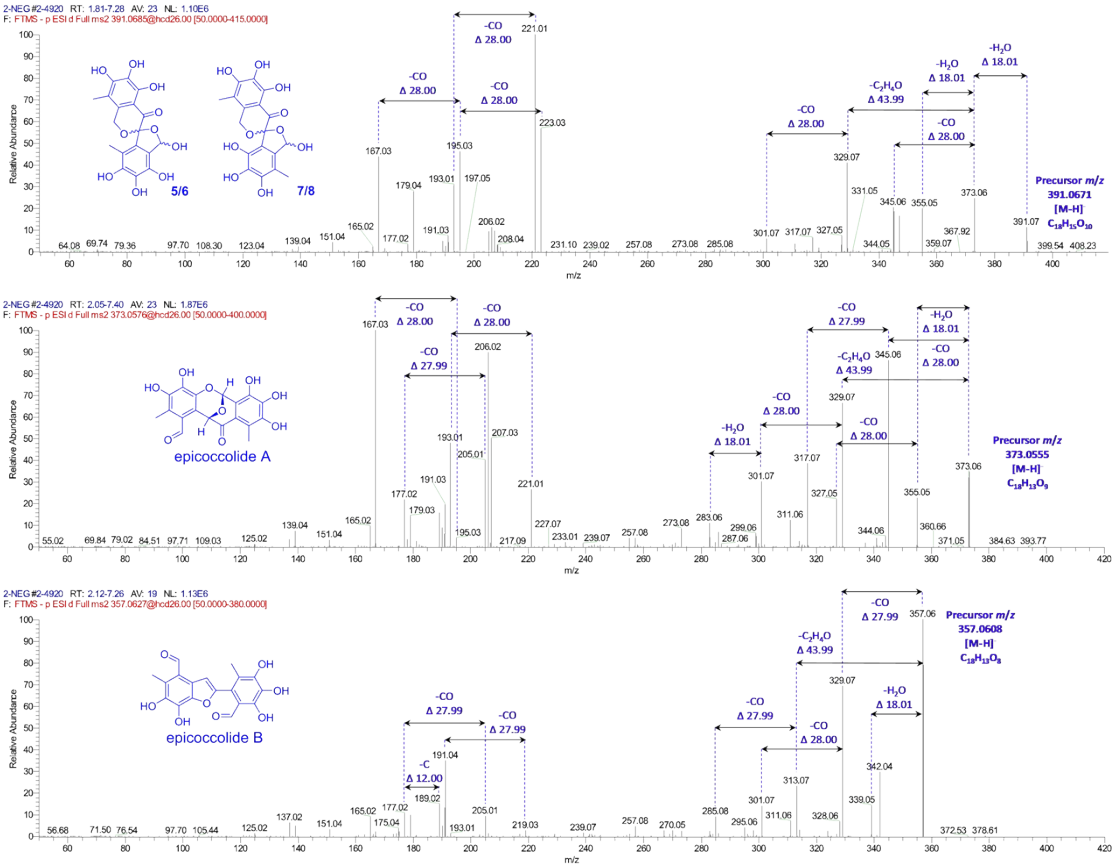

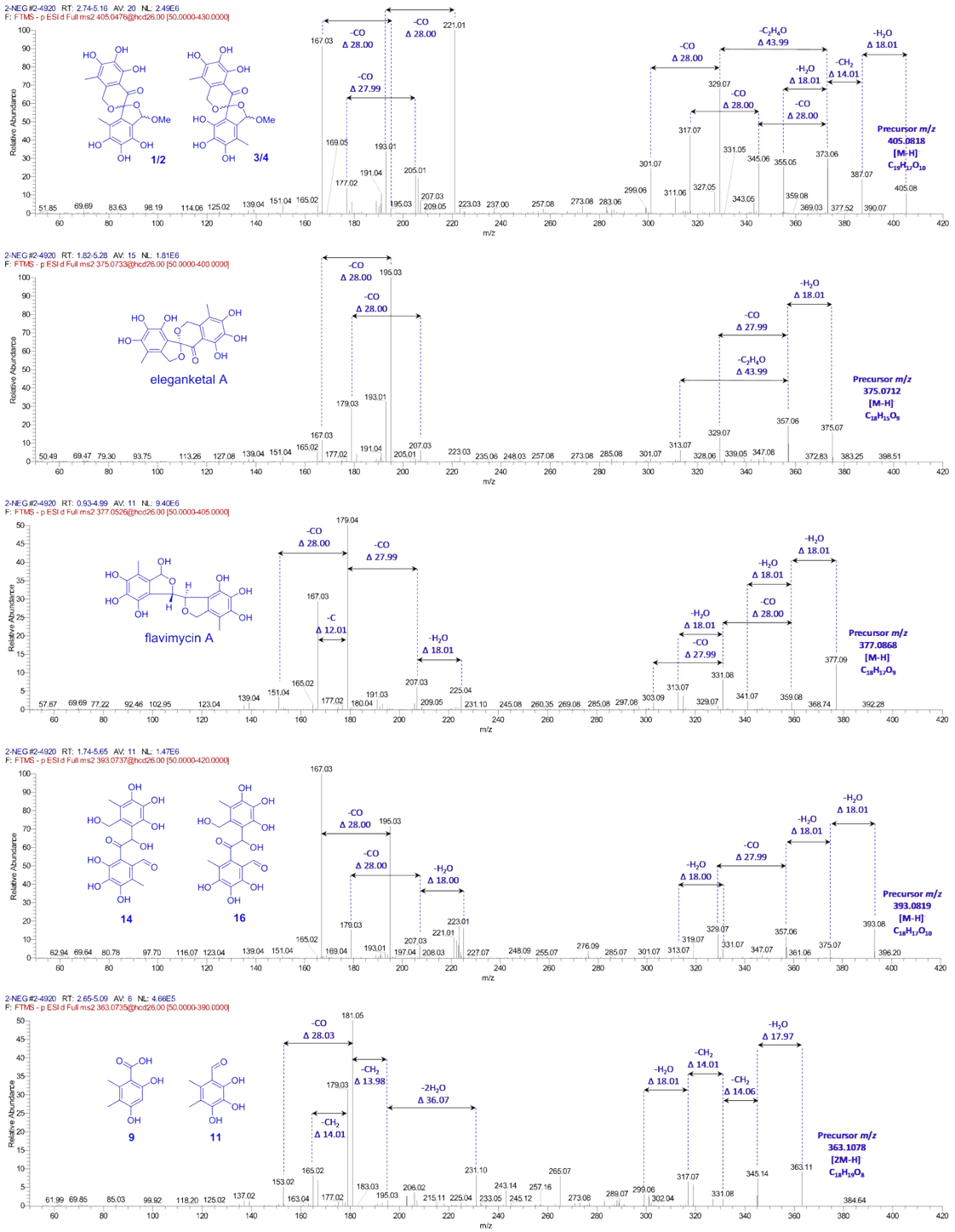

Fig. S2 Tandem MS/MS (performed on Thermal Q Exactive orbitrap MS system) fragmentation of annotated compounds in Cluster I.

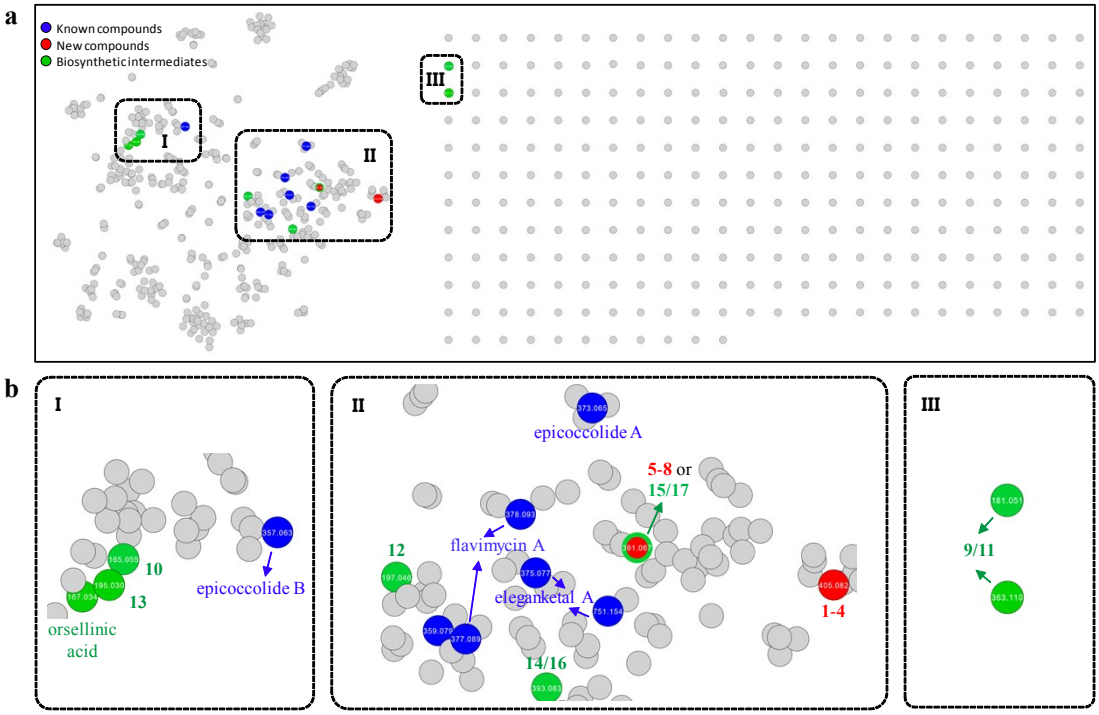

Fig. S3 Molecular networking generated by MetGem software based on the t-SNE Algorithm. (a) Over view of the t-SNE graph. Known compounds, new compounds and biosynthetic intermediates are marked with blue, red, green circles, respectively. (b) Zoomed view of area I, II, III.

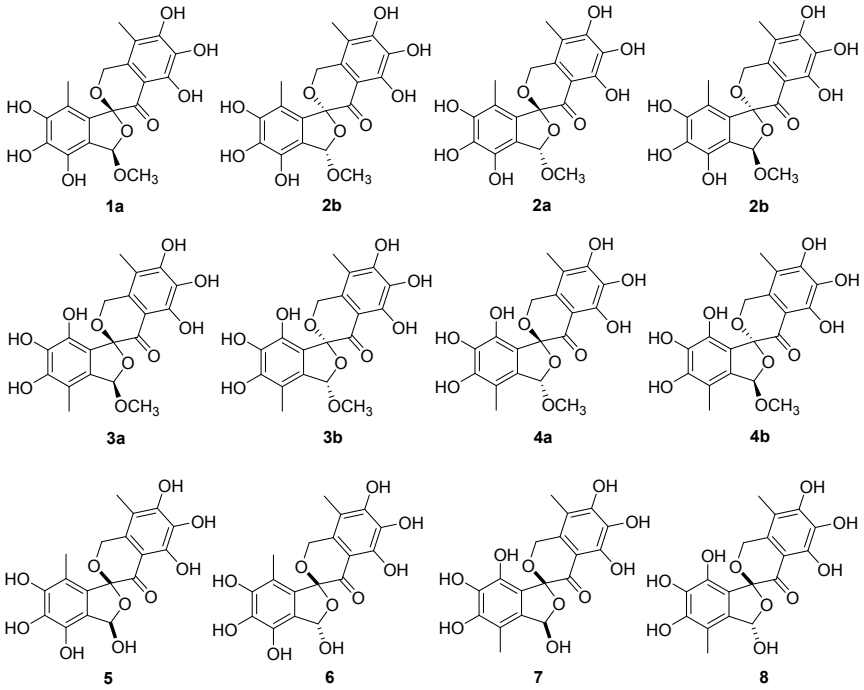

Fig. S4 Full structures of epicospirocins (**1**−**8**).

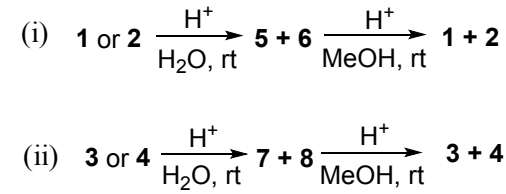

Fig. S5 Non-enzymatic conversion of epicospirocins.

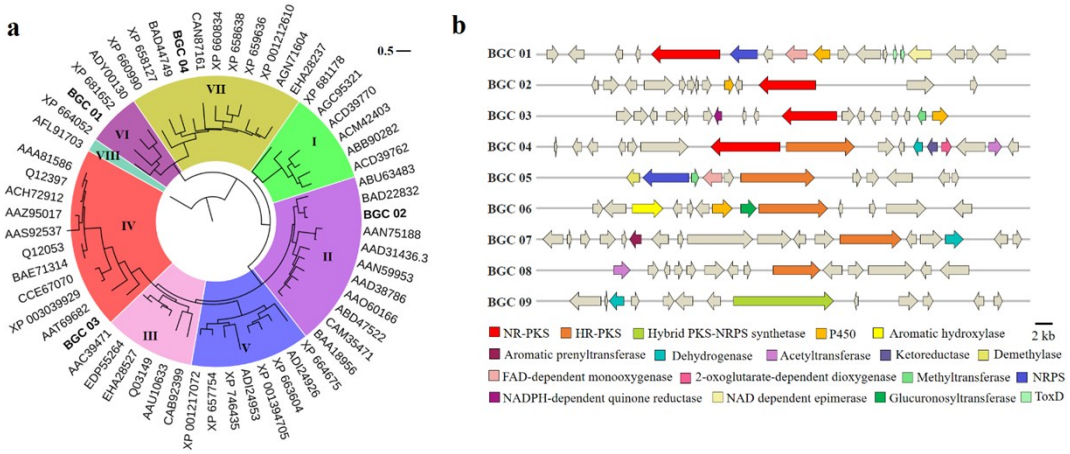

Fig. S6 Phylogenetic analysis of product template (PT) domain of NR-PKSs.
(a) Maximum likelihood phylogenetic tree of PT domains of 4 (putative) NR-PKSs found in EN09116 and 55 Previously characterized NR-PKSs that have been summarized in Supplementary Table S6. (b) Gene organization of biosynthetic gene clusters containing PKS gene from EN09116.

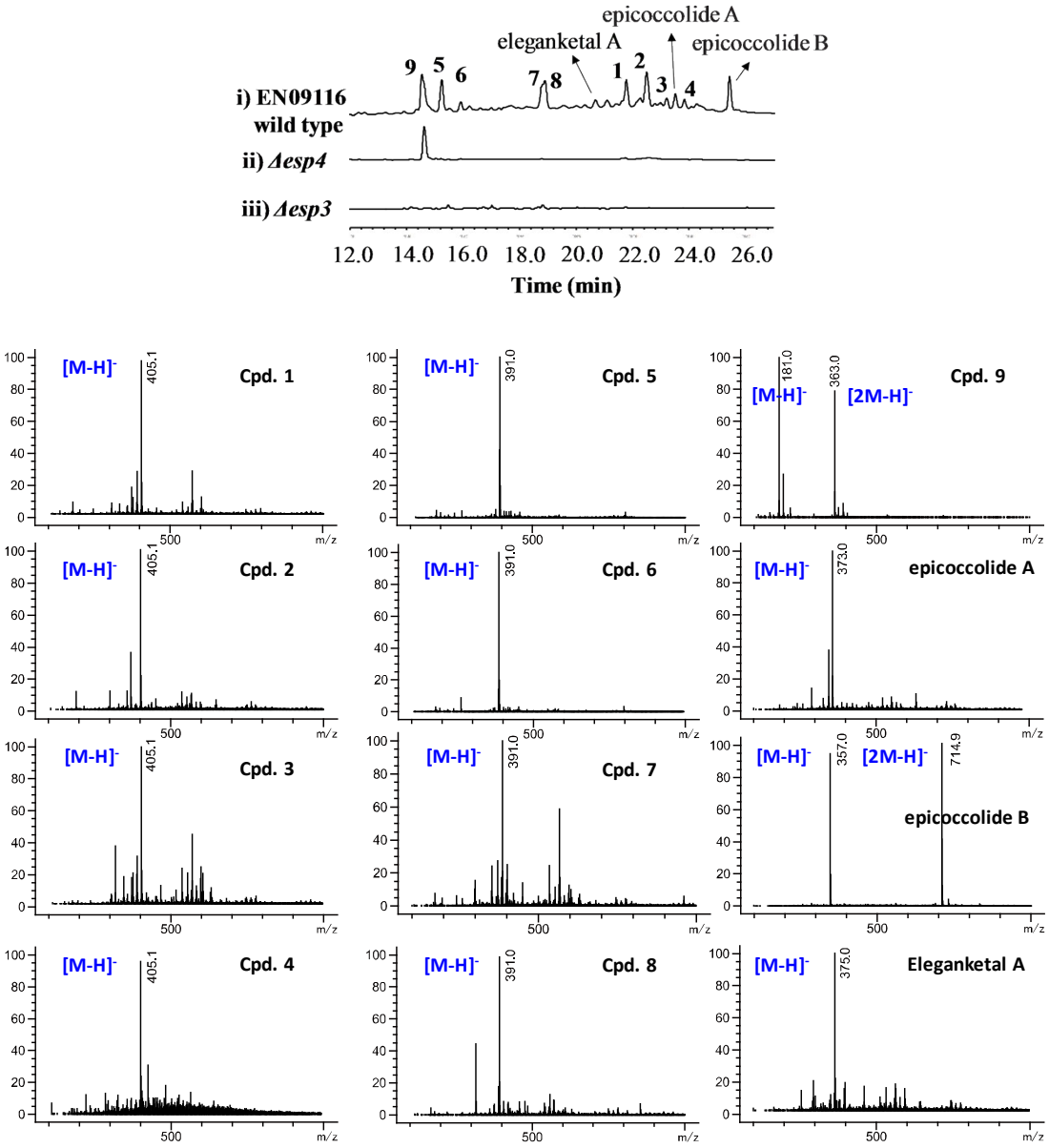

Fig. S7 LC-MS profiles (UV at 230 nm, *m/z* 50-1000) of metabolites extracted from EN09116 wild-type and mutant strains

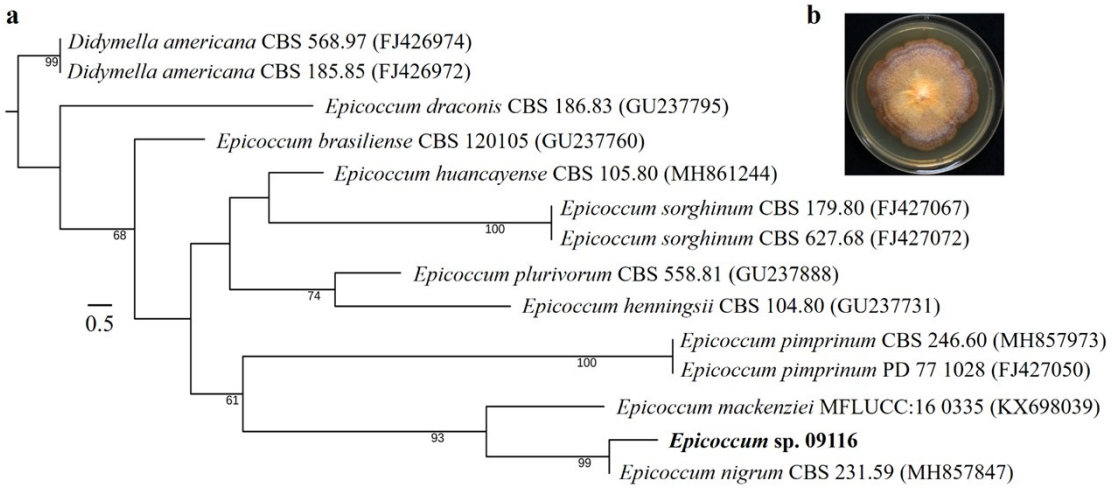

Fig. S8 Morphology and phylogenetic tree of EN09116.
(**a**) Neighbor-joining tree of EN09116 based on 18S sequences. Numbers at nodes indicate levels of bootstrap support (%) based on a neighbor-joining analysis of 1000 resampled datasets; only values > 50% are shown. The tree is rooted to Didymella americana (CBS 568.97; CBS 185.85). NCBI accession numbers are provided in parentheses. The bar represents 0.5 nucleotide substitutions per site. (**b**) Colony characteristics of EN09116 grown on potato dextrose agar at 28℃ for 10 days.

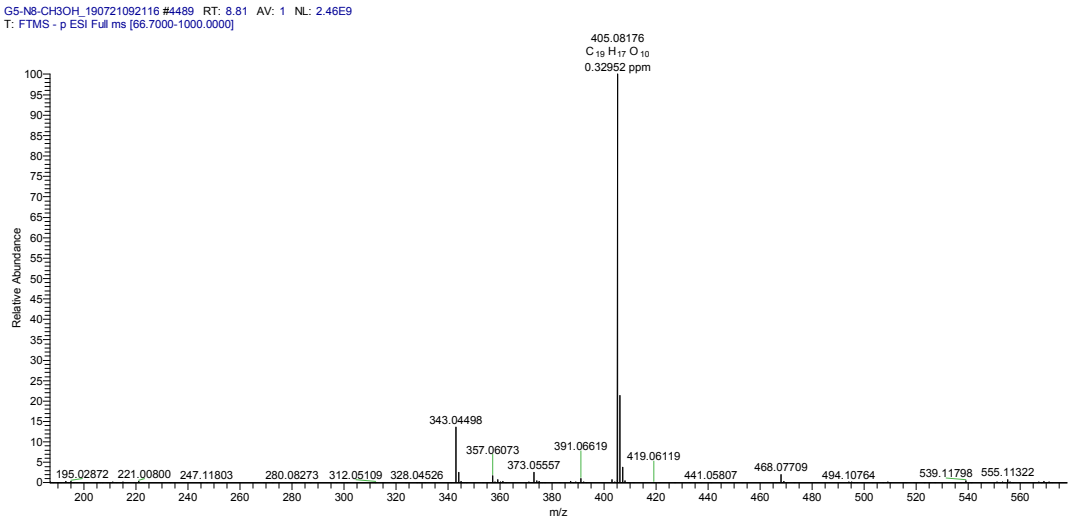

Fig. S9 HR-ESI-MS spectrum of **1a/1b**

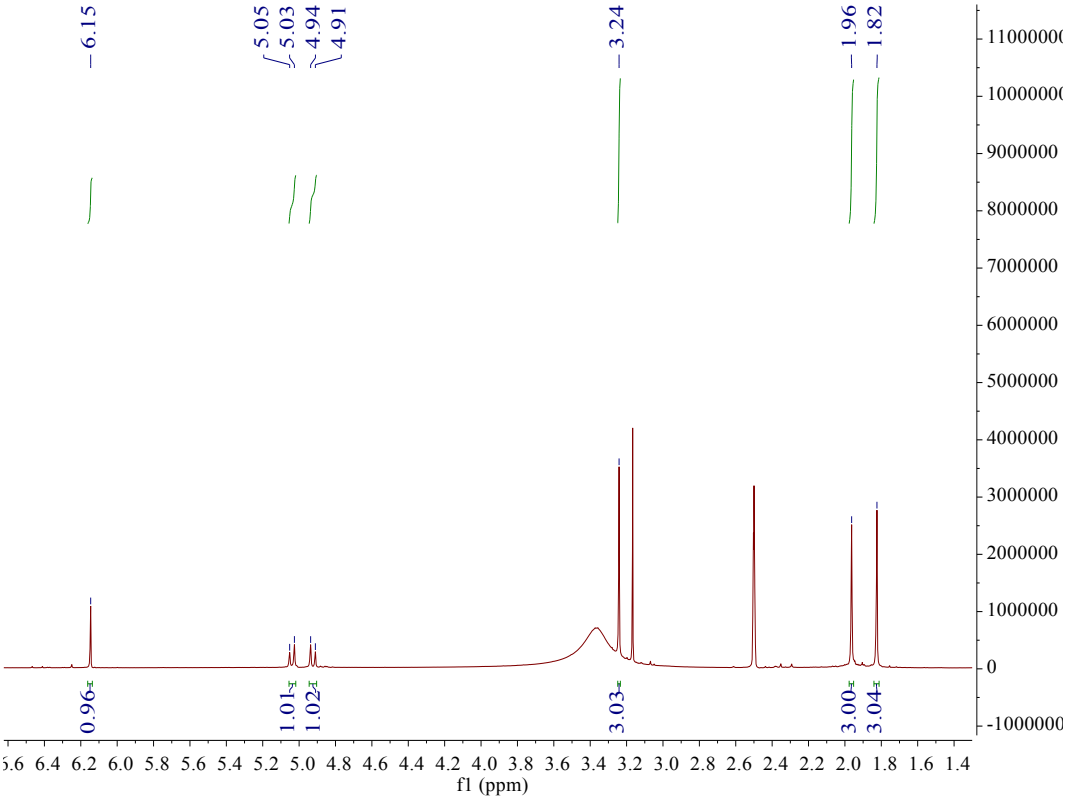

Fig. S10 ^{1}H NMR (600 MHz, DMSO-d_6) spectra of **1a**/**1b**

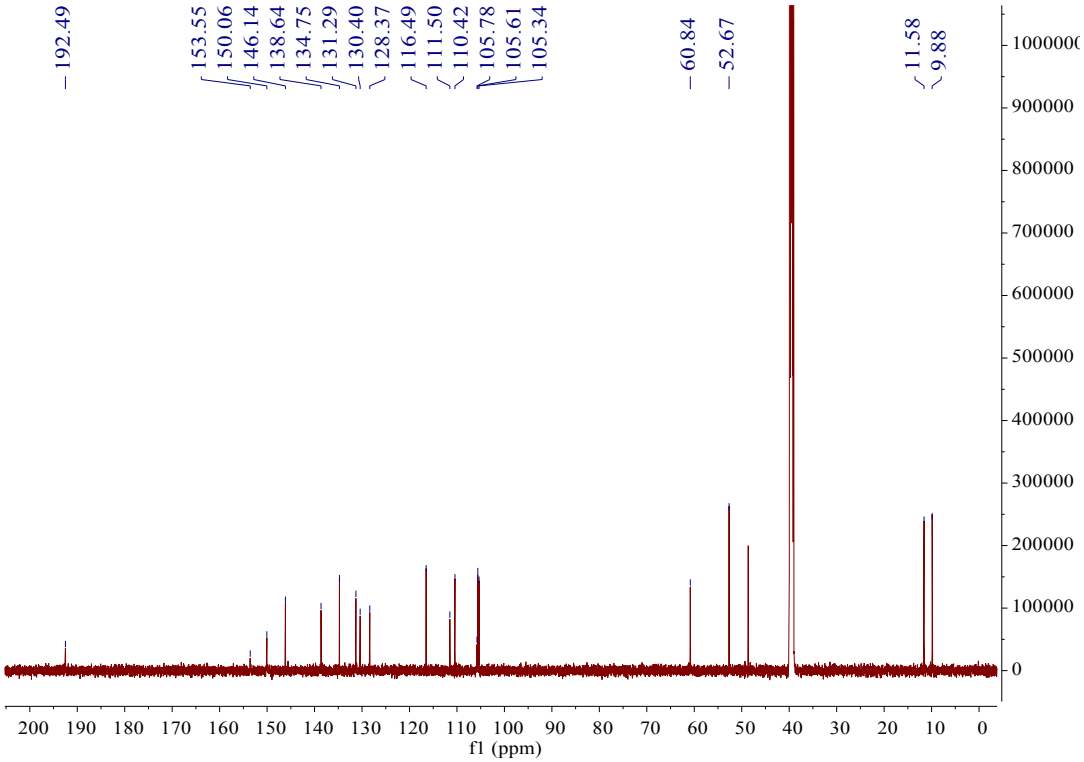

Fig. S11 ^{13}C NMR (150 MHz, DMSO-d_6) spectra of **1a**/**1b**

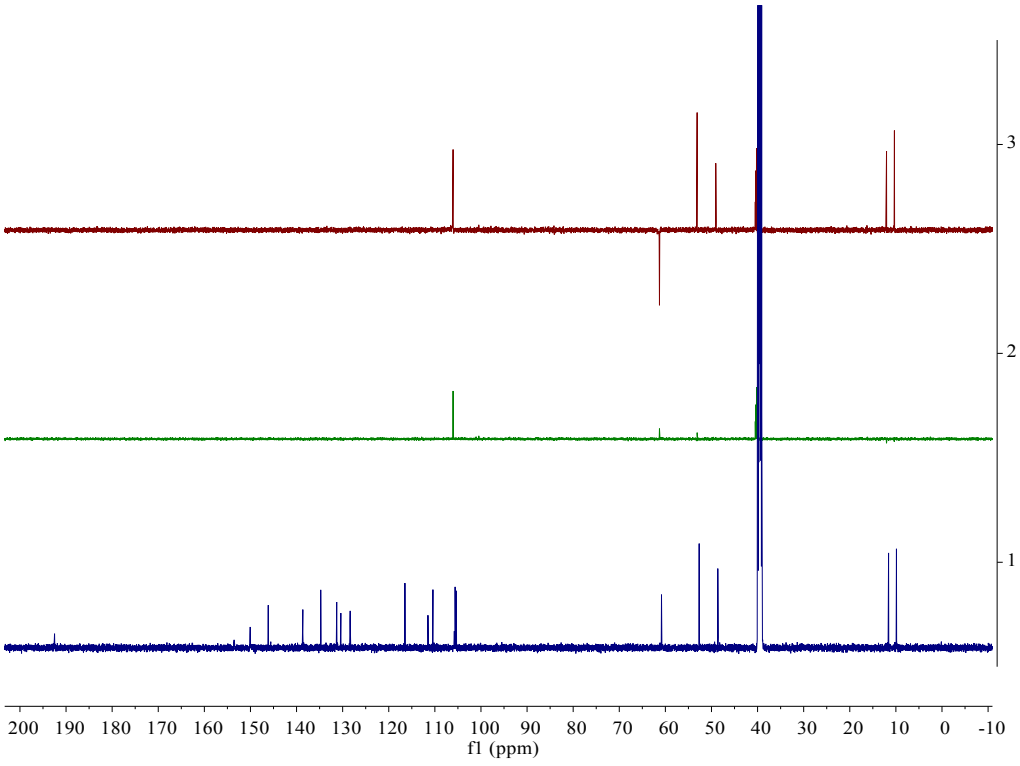

Fig. S12 DEPT NMR (150 MHz, DMSO-d_6) spectrum of **1a**/**1b**

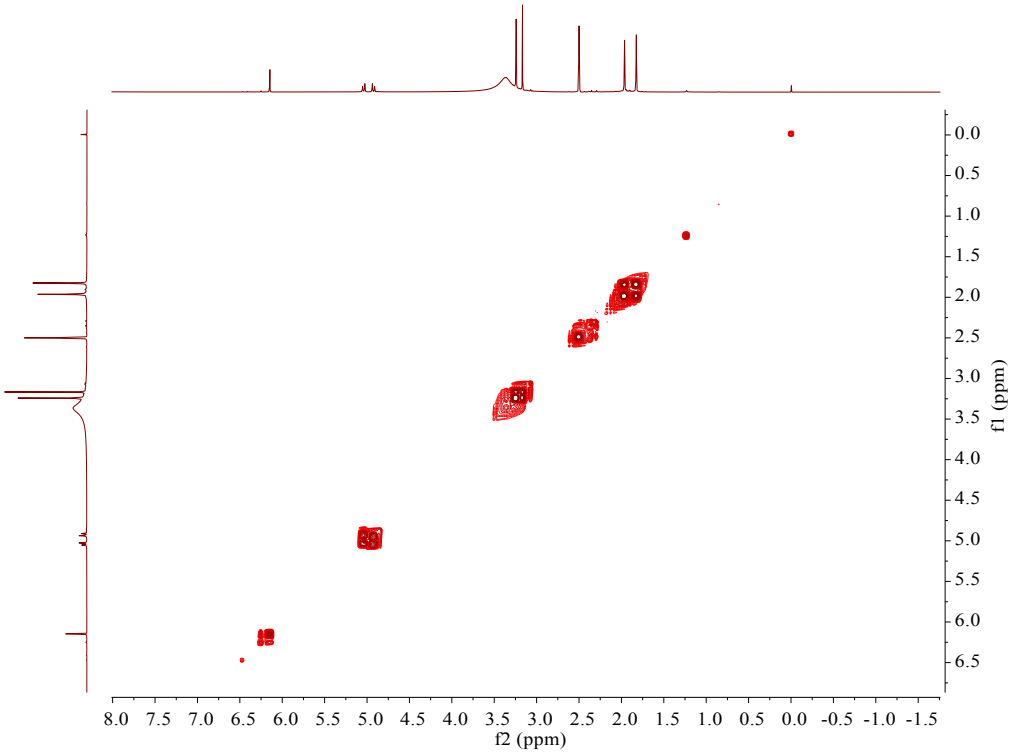

Fig. S13 ^{1}H-^{1}H COSY NMR (600 MHz, DMSO-d_6) spectrum of **1a**/**1b**

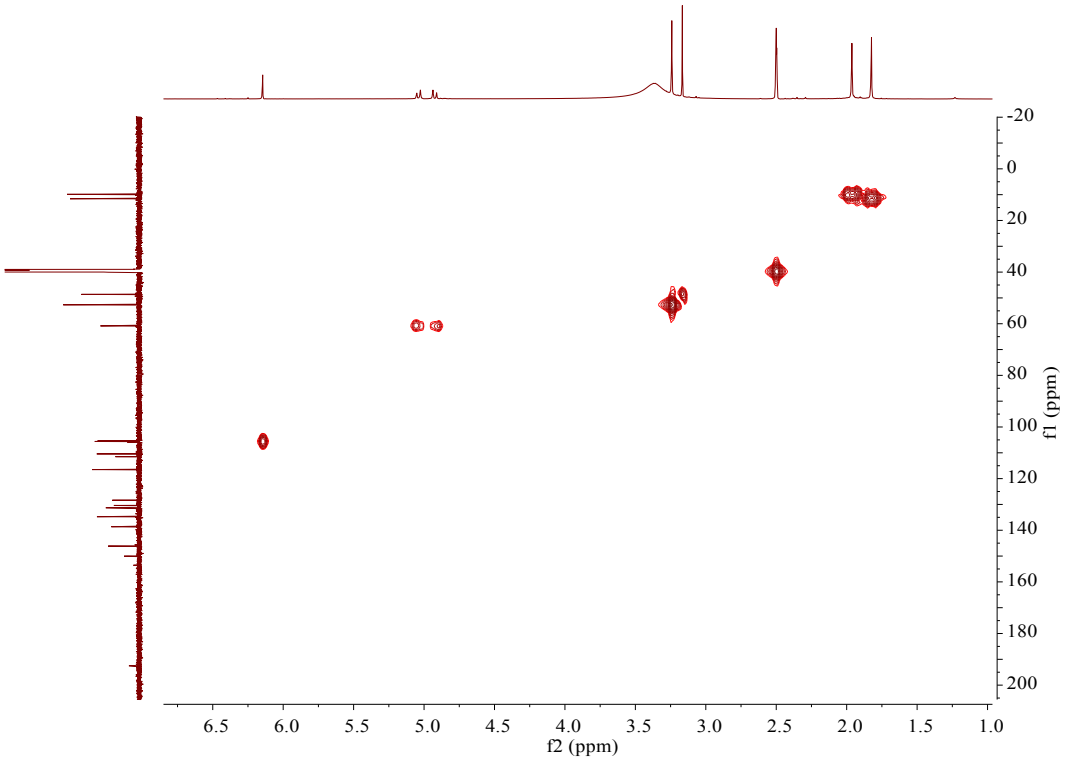

Fig. S14 HSQC NMR (600 MHz, DMSO-d_6) spectrum of **1a**/**1b**

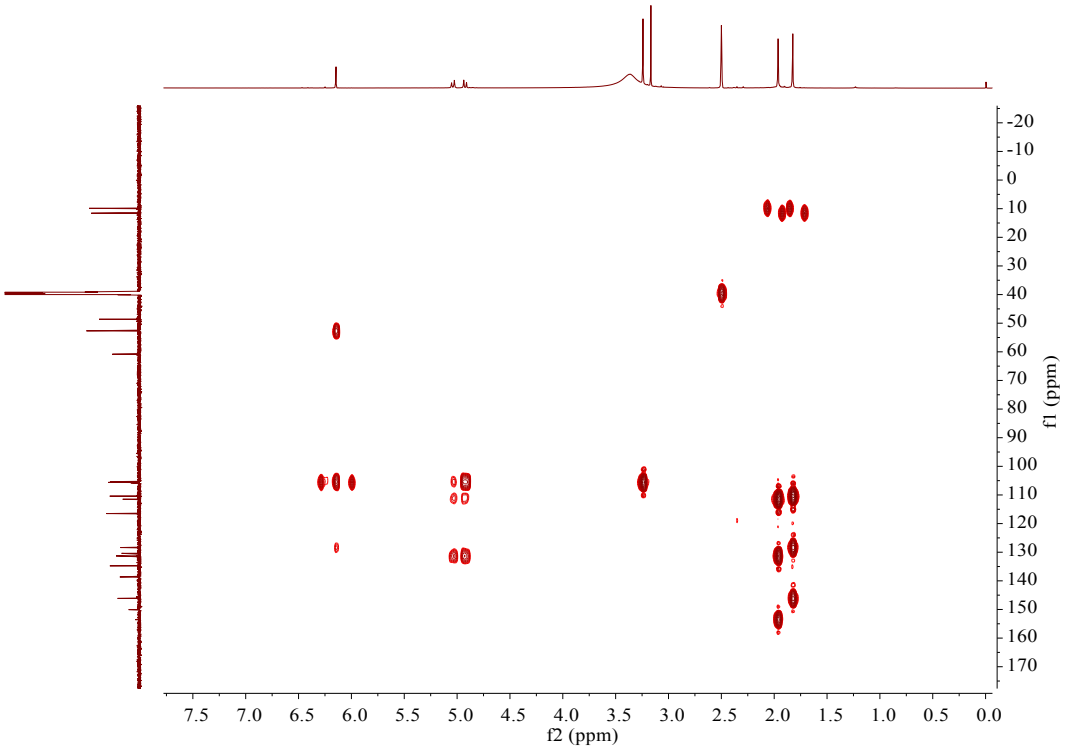

Fig. S15 HMBC NMR (600 MHz, DMSO-d_6) spectrum of **1a**/**1b**

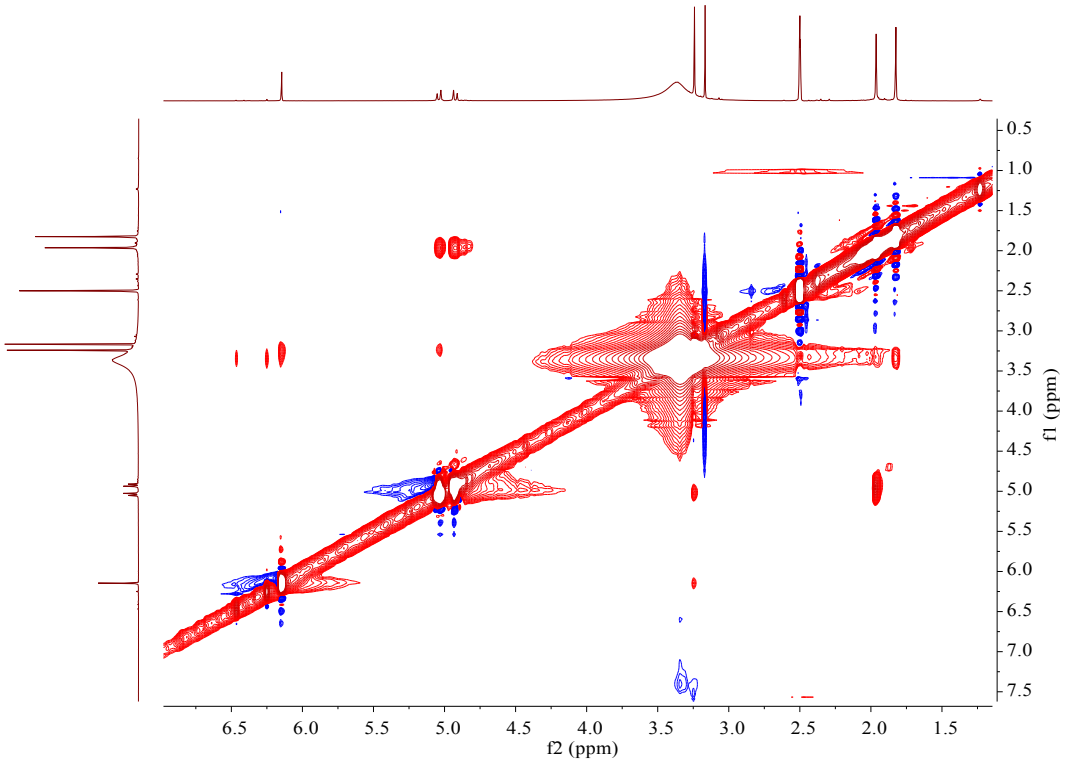

Fig. S16 NOESY NMR (600 MHz, DMSO-d_6) spectrum of **1a**/**1b**

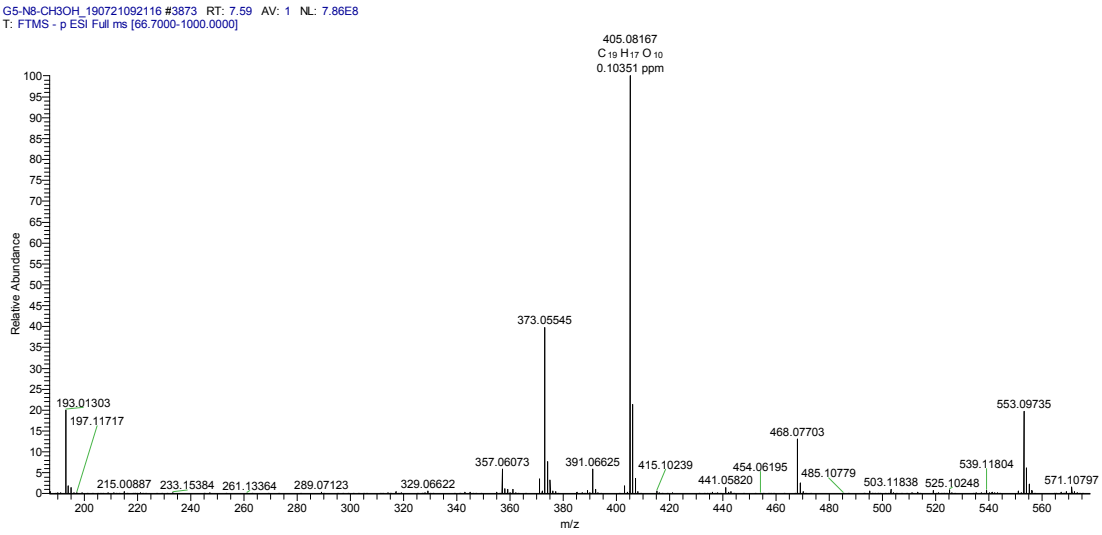

Fig. S17 HR-ESI-MS spectrum of **2a/2b**

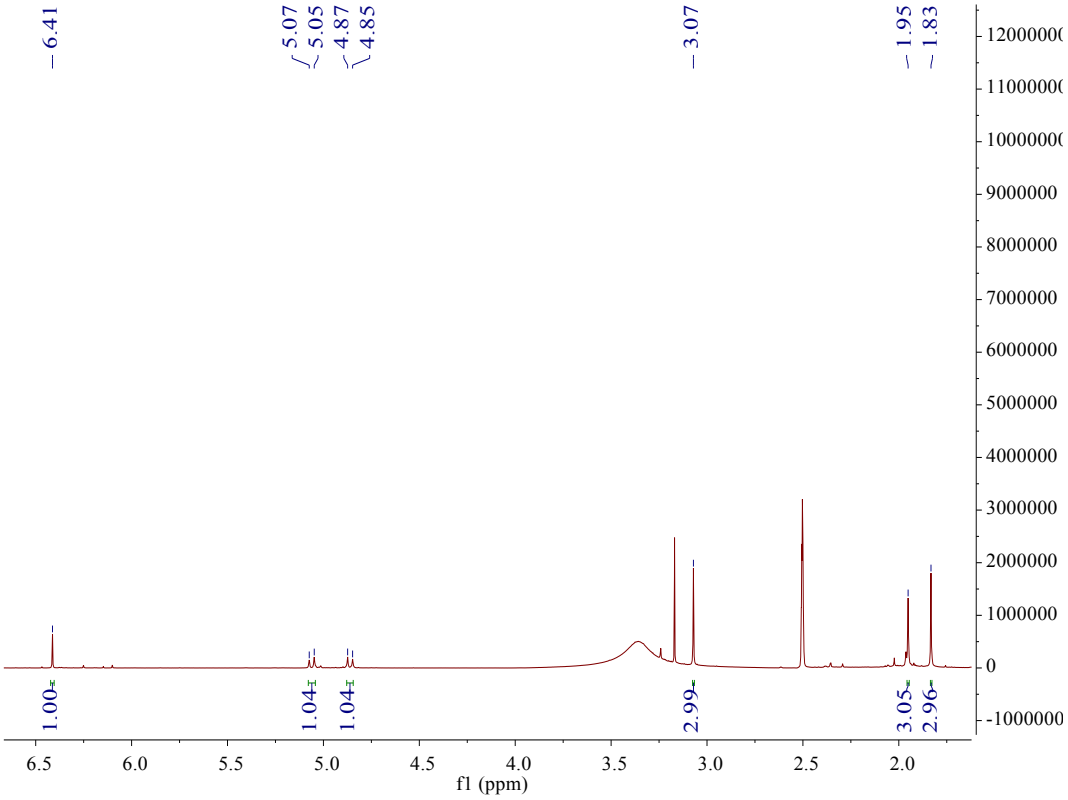

Fig. S18 ^{1}H NMR (600 MHz, DMSO-d_6) spectra of **2a**/**2b**

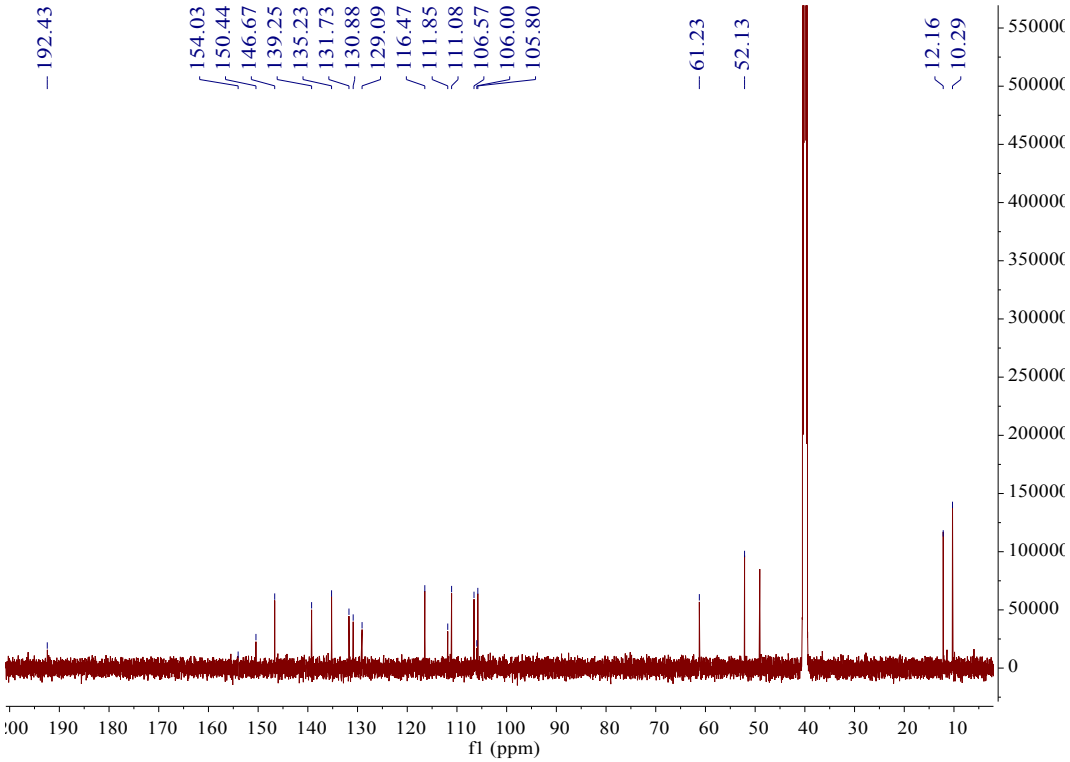

Fig. S19 ^{13}C NMR (150 MHz, DMSO-d_6) spectra of **2a**/**2b**

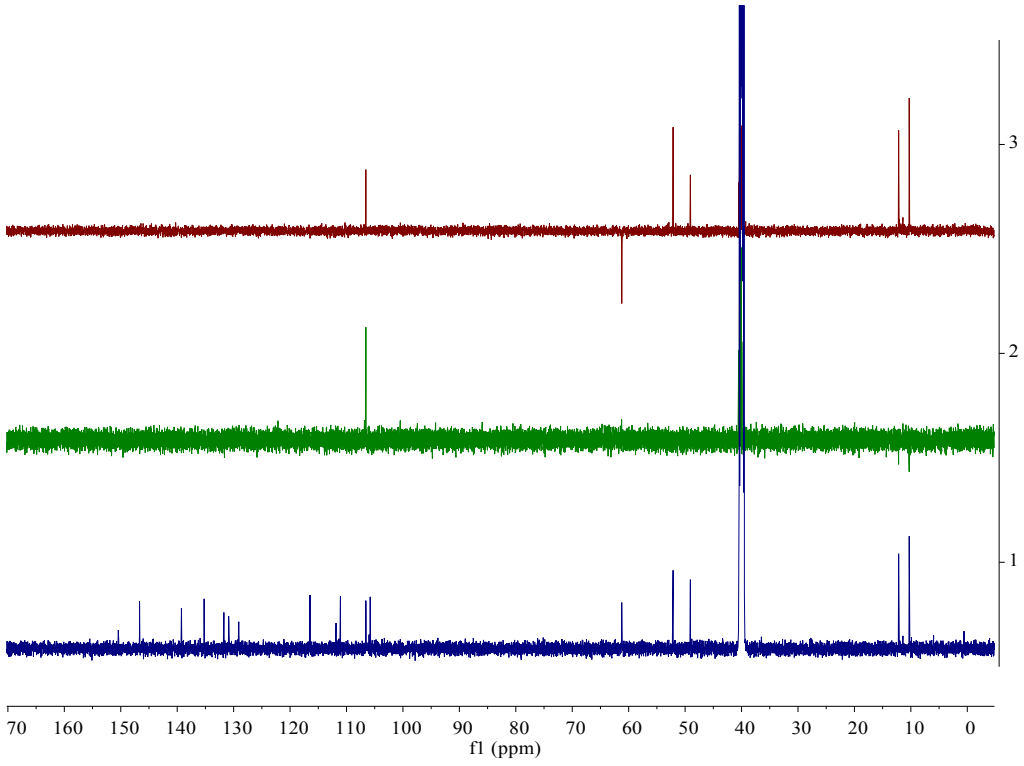

Fig. S20 DEPT NMR (150 MHz, DMSO-d_6) spectra of **2a**/**2b**

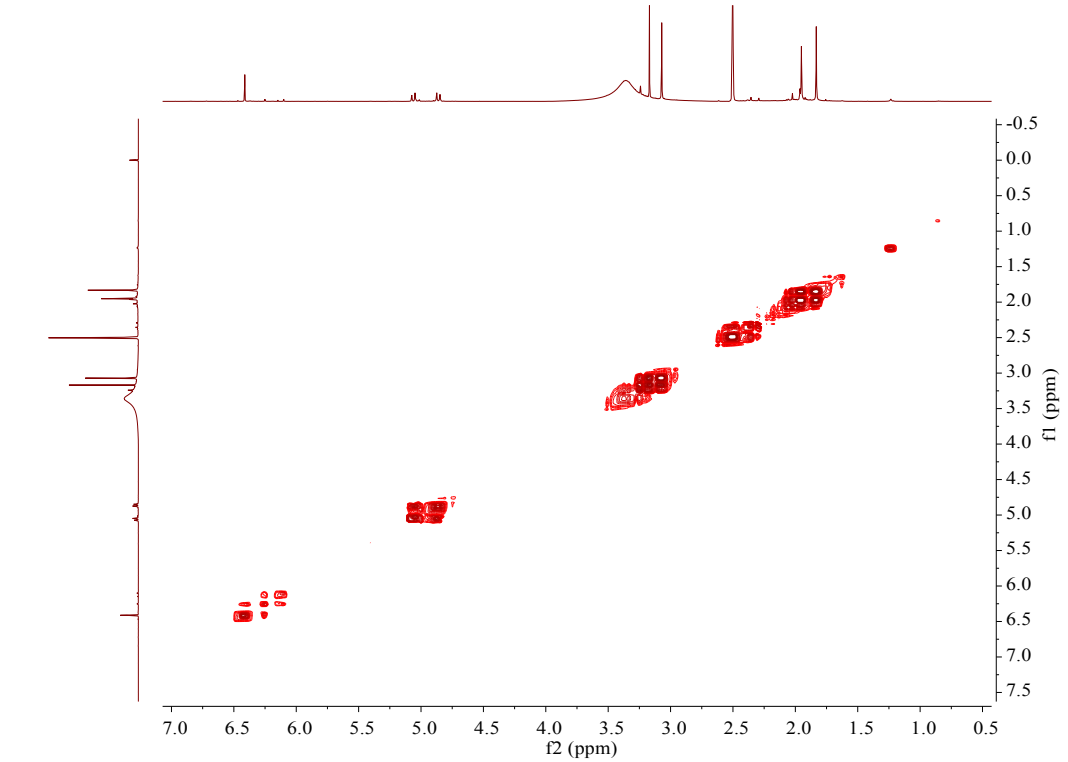

Fig. S21 ^{1}H-^{1}H COSY NMR (600 MHz, DMSO-d_6) spectrum of **2a**/**2b**

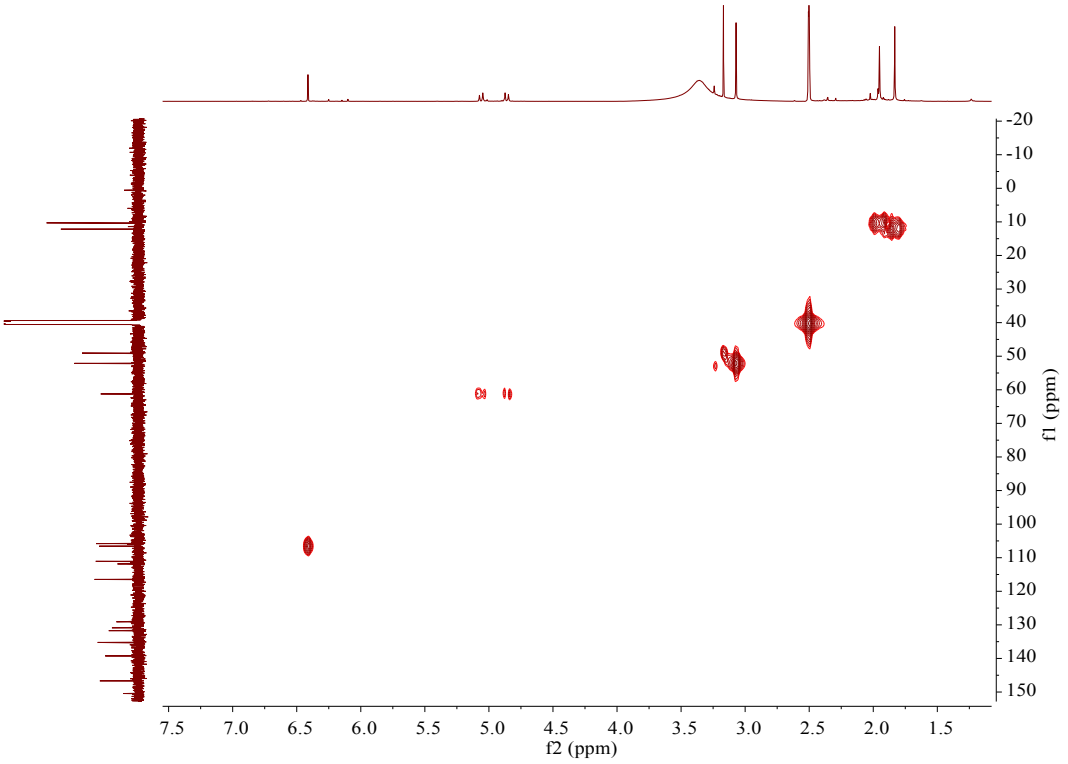

Fig. S22 HSQC NMR (600 MHz, DMSO-d_6) spectrum of **2a**/**2b**

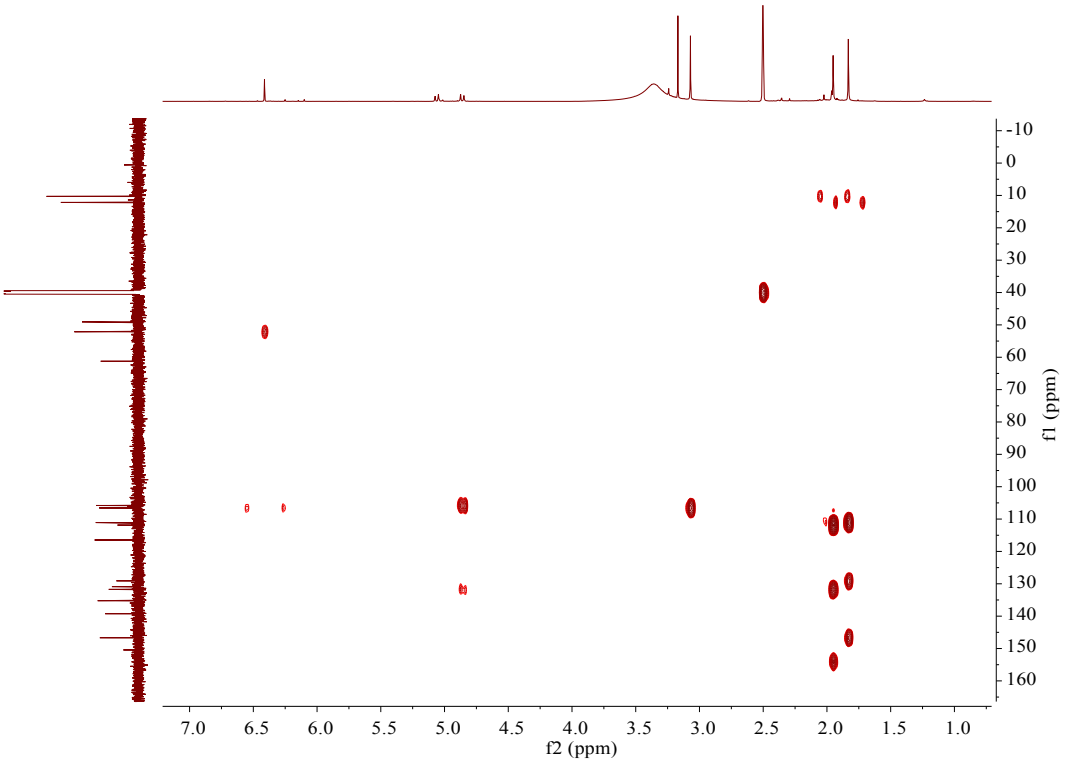

Fig. S23 HMBC NMR (600 MHz, DMSO-d_6) spectrum of **2a**/**2b**

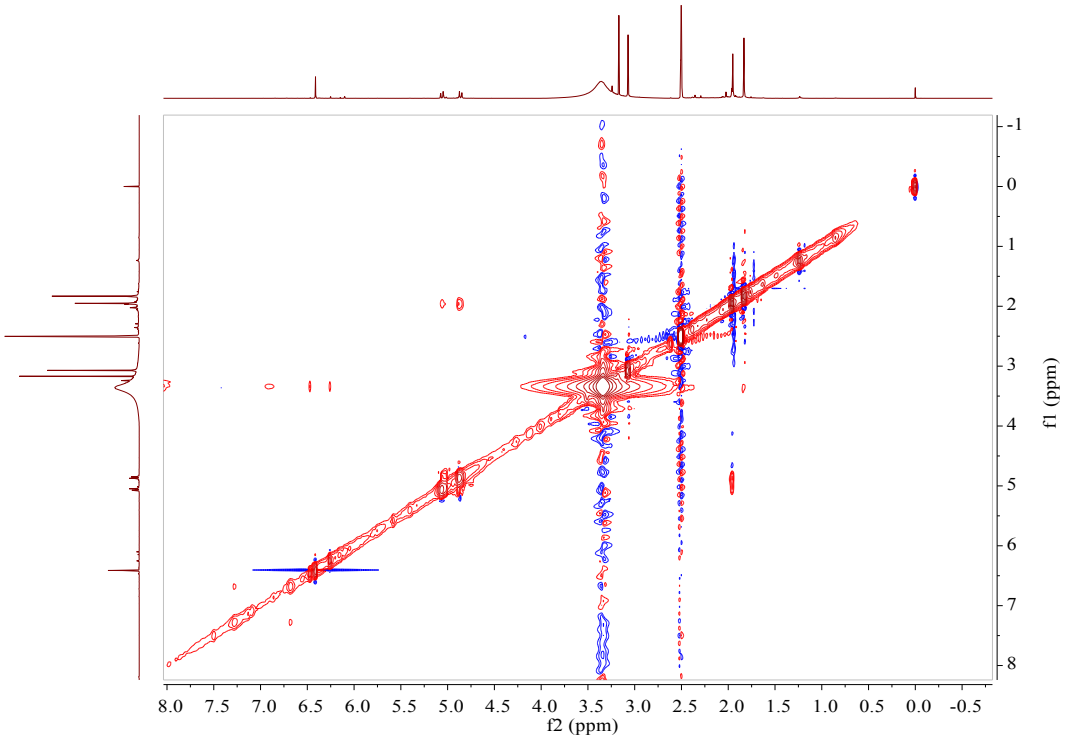

Fig. S24 NOESY NMR (600 MHz, DMSO-d_6) spectrum of **2a**/**2b**

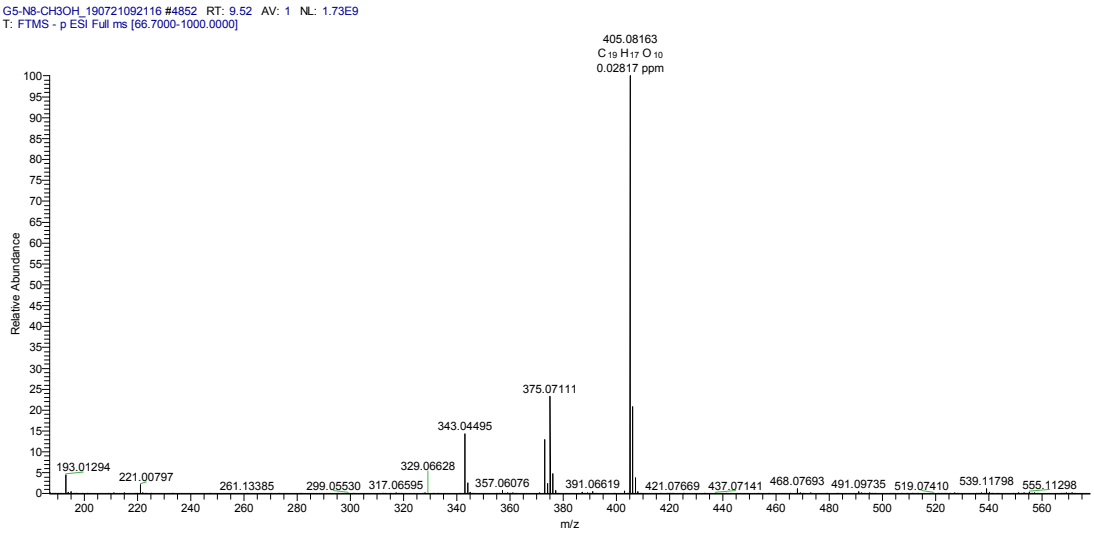

Fig. S25 HR-ESI-MS spectrum of **3a/3b**

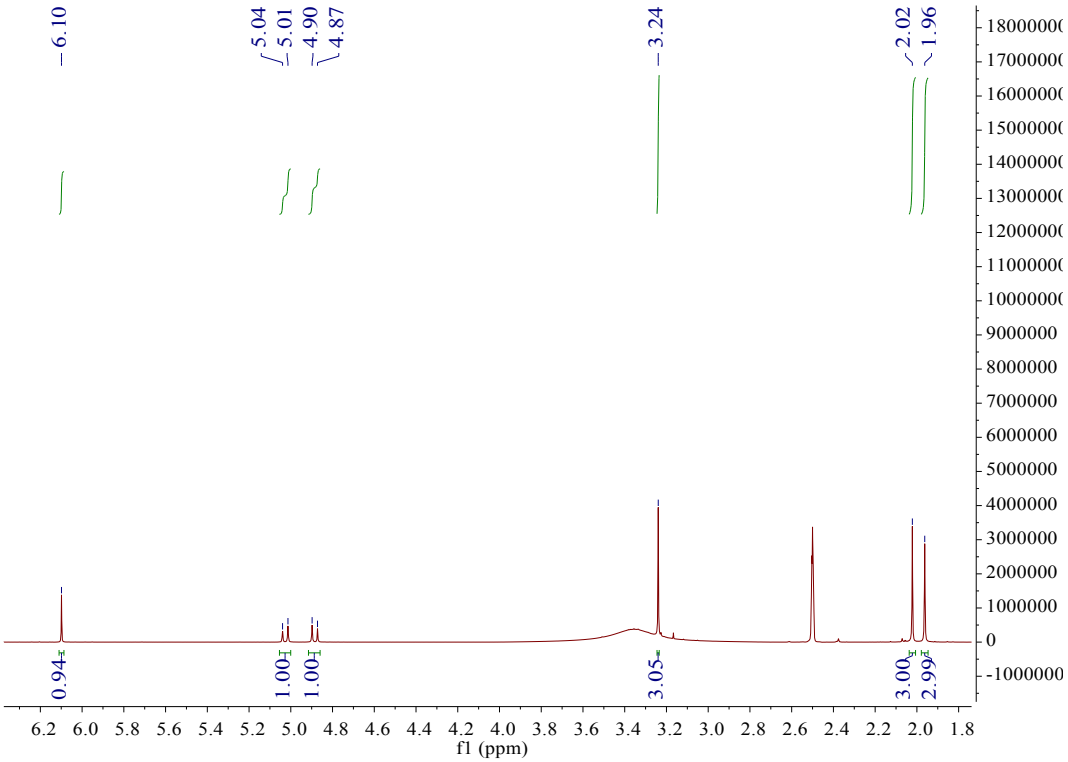

Fig. S26 ^{1}H NMR (600 MHz, DMSO-d_6) spectra of **3a**/**3b**

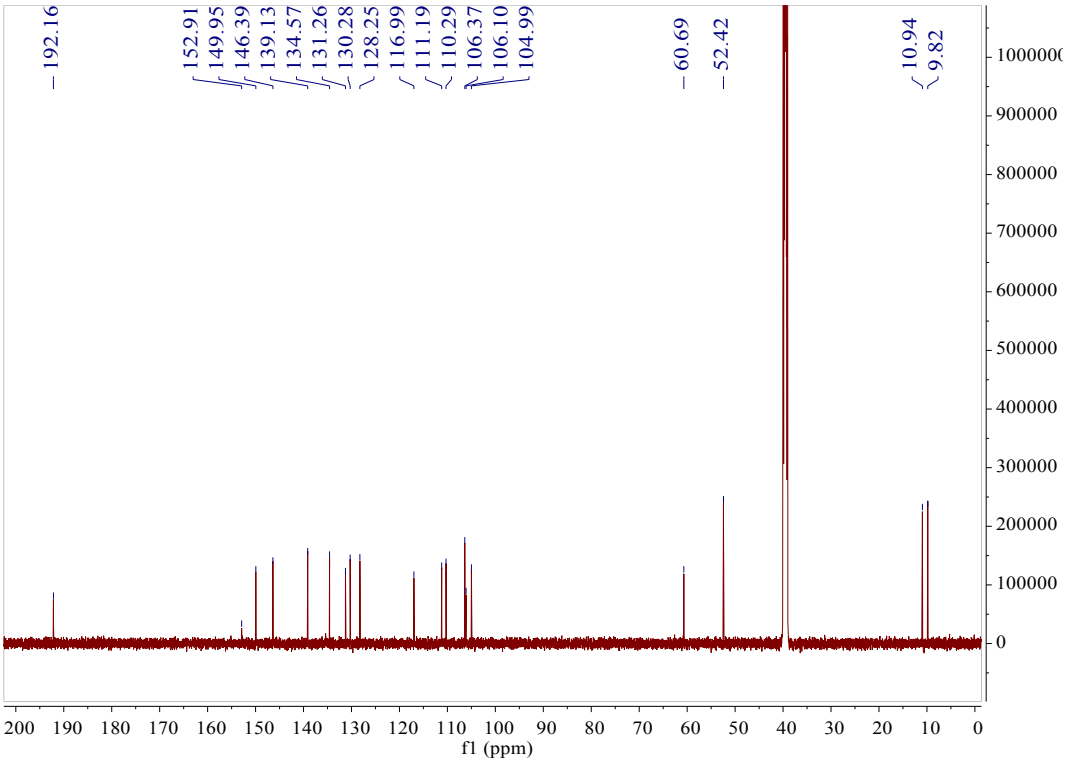

Fig. S27 ^{13}C NMR (150 MHz, DMSO-d_6) spectra of **3a**/**3b**

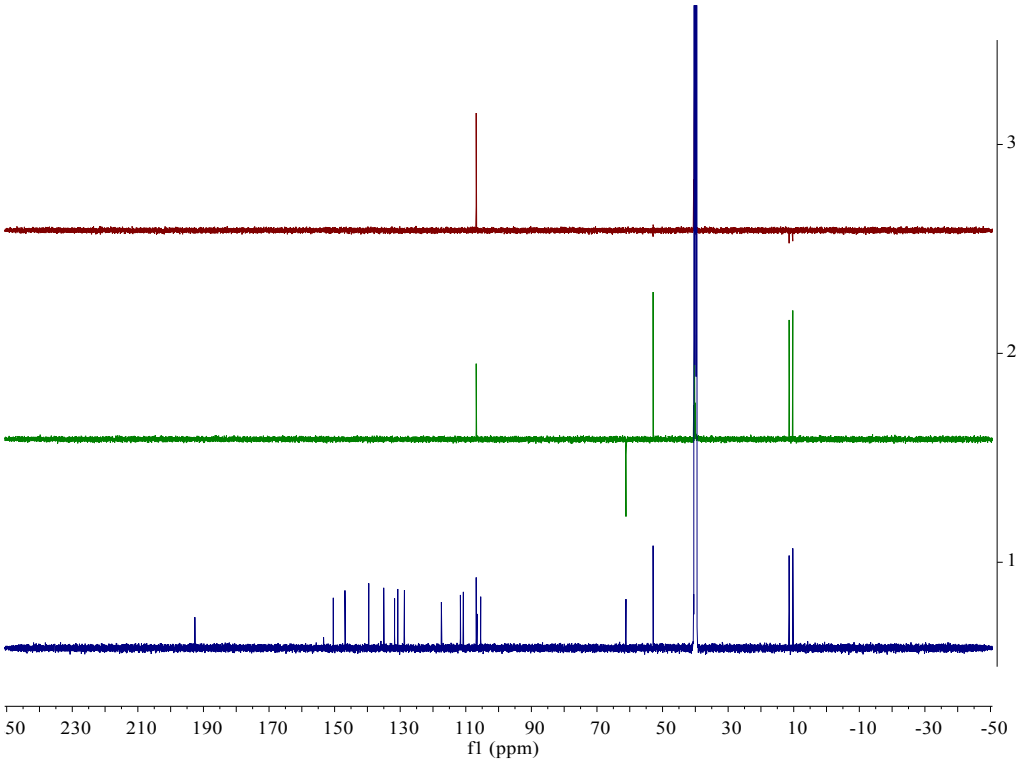

Fig. S28 DEPT NMR (150 MHz, DMSO-d_6) spectra of **3a**/**3b**

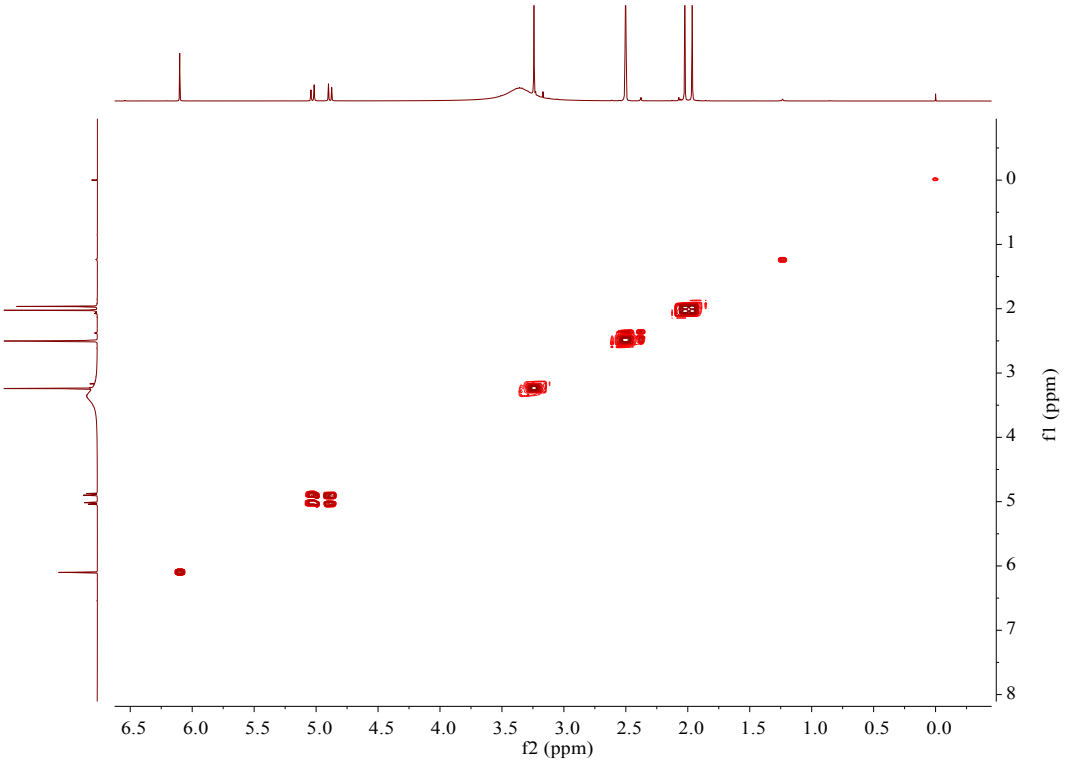

Fig. S29 ^{1}H-^{1}H COSY NMR (600 MHz, DMSO-d_6) spectrum of **3a**/**3b**

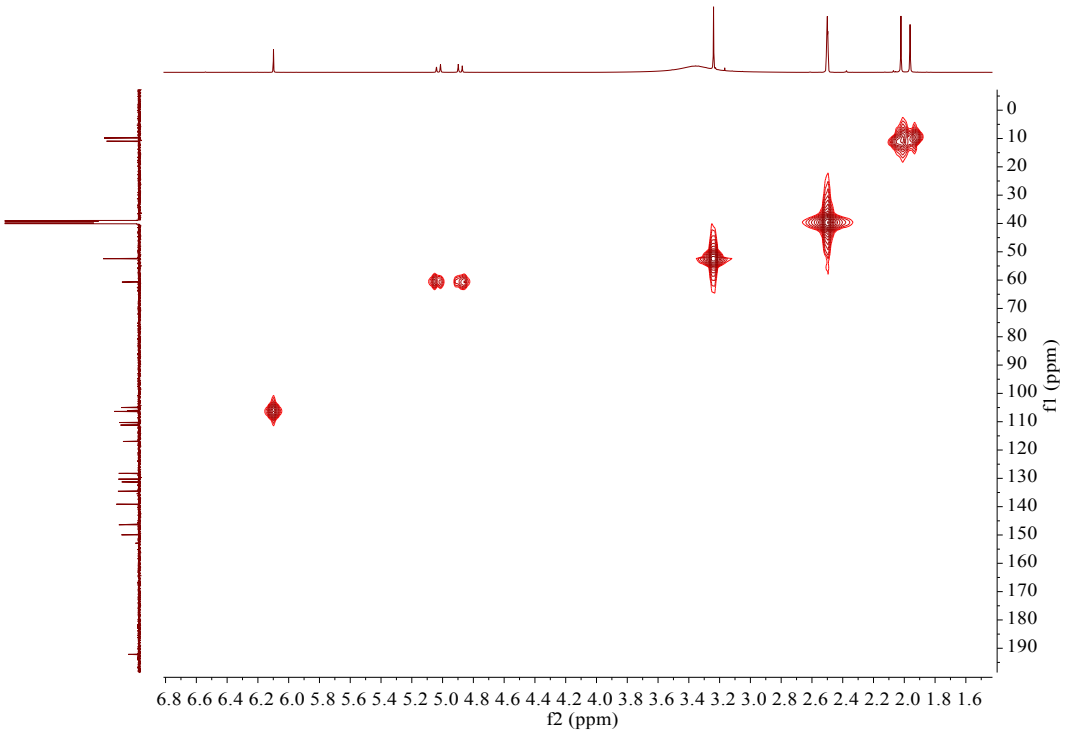

Fig. S30 HSQC NMR (600 MHz, DMSO-d_6) spectrum of **3a**/**3b**

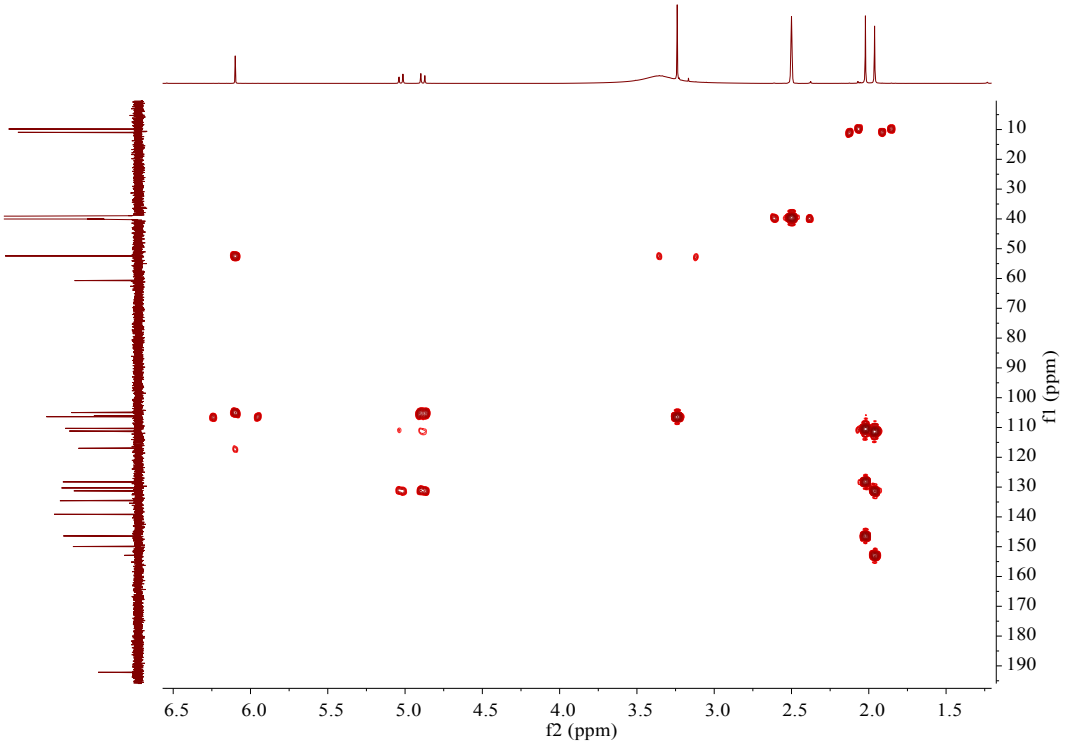

Fig. S31 HMBC NMR (600 MHz, DMSO-d_6) spectrum of **3a**/**3b**

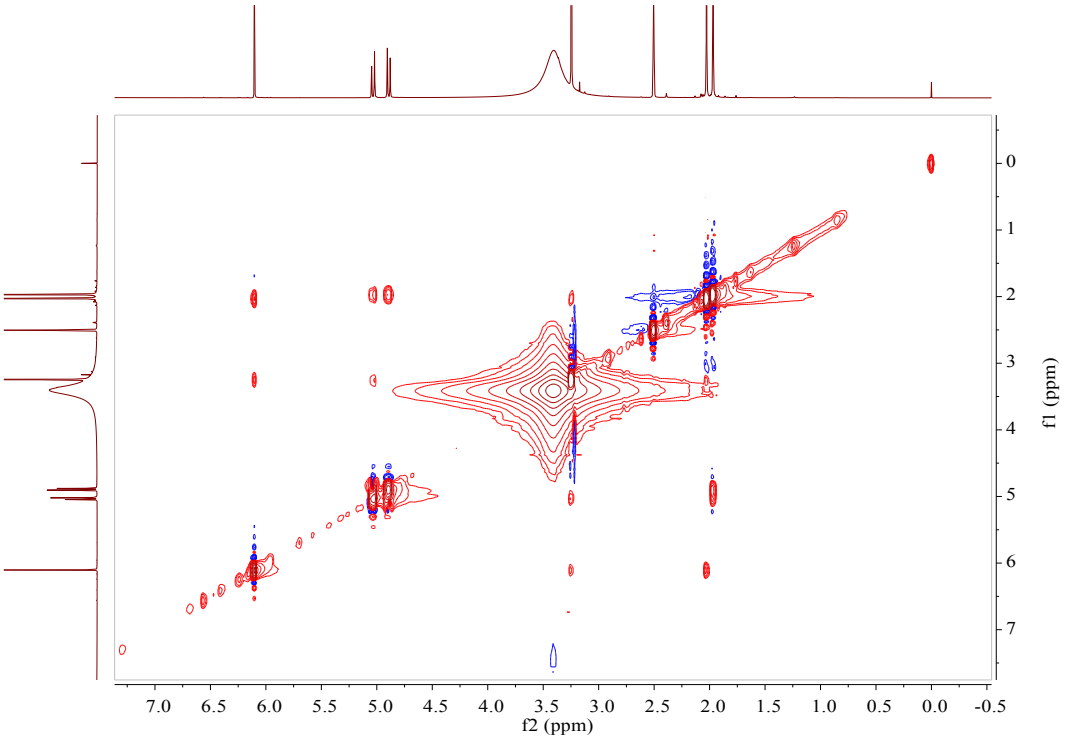

Fig. S32 NOESY NMR (600 MHz, DMSO-d_6) spectrum of **3a**/**3b**

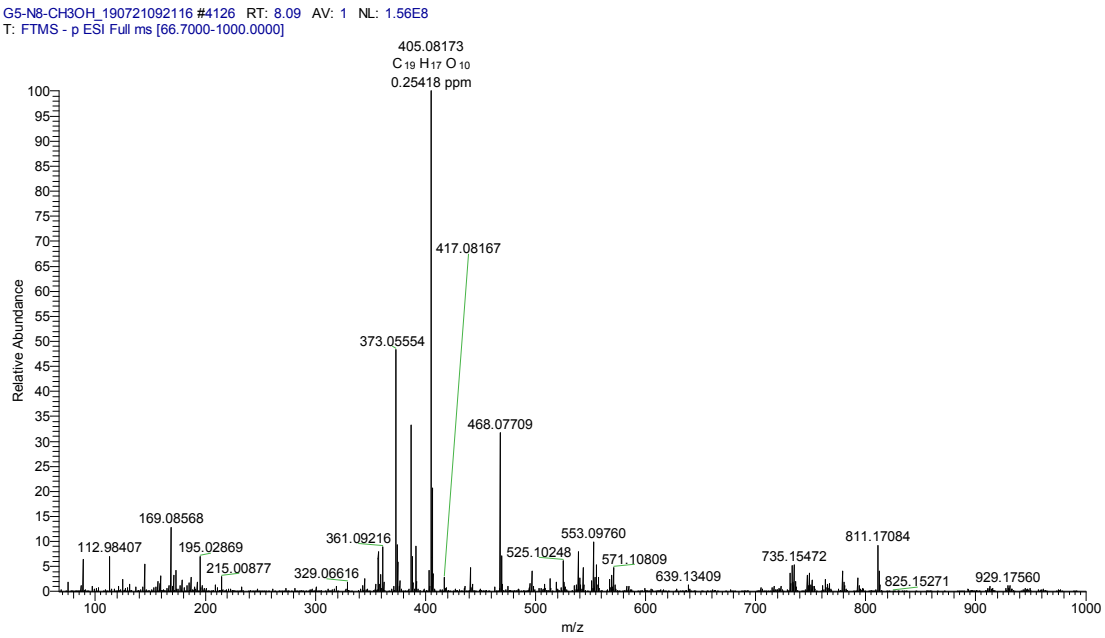

Fig. S33 HR-ESI-MS spectrum of **4a/4b**

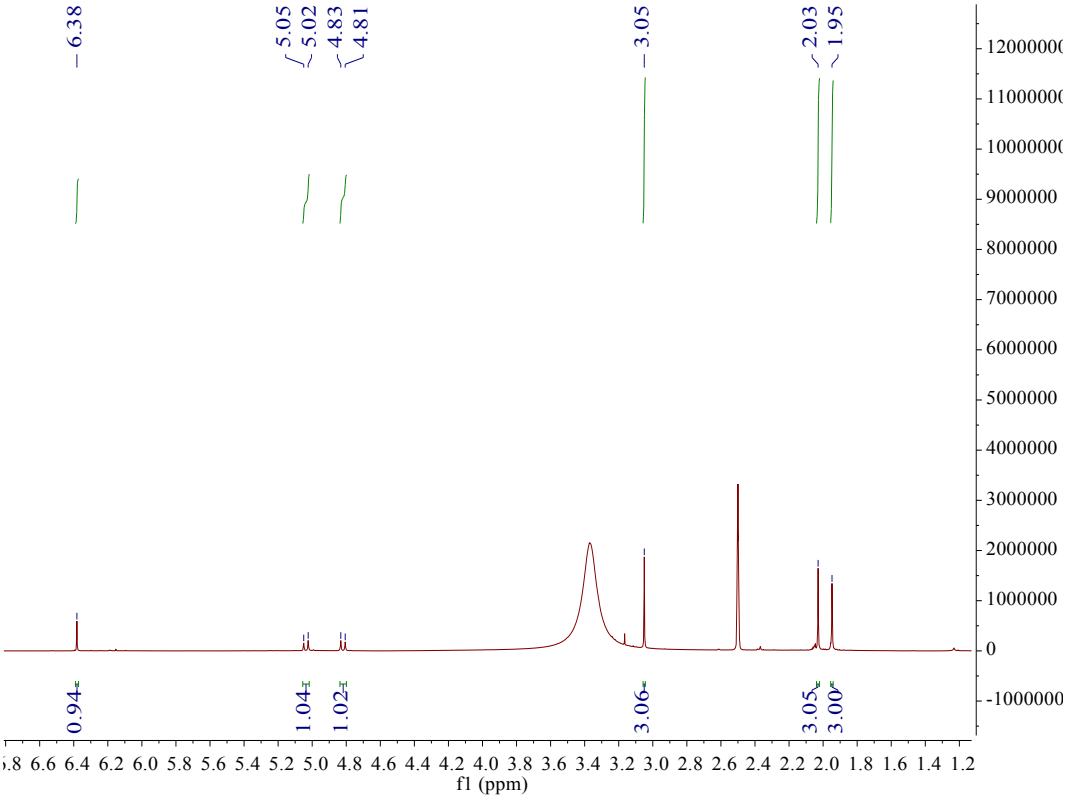

Fig. S34 ^{1}H NMR (600 MHz, DMSO-d_6) spectra of **4a**/**4b**

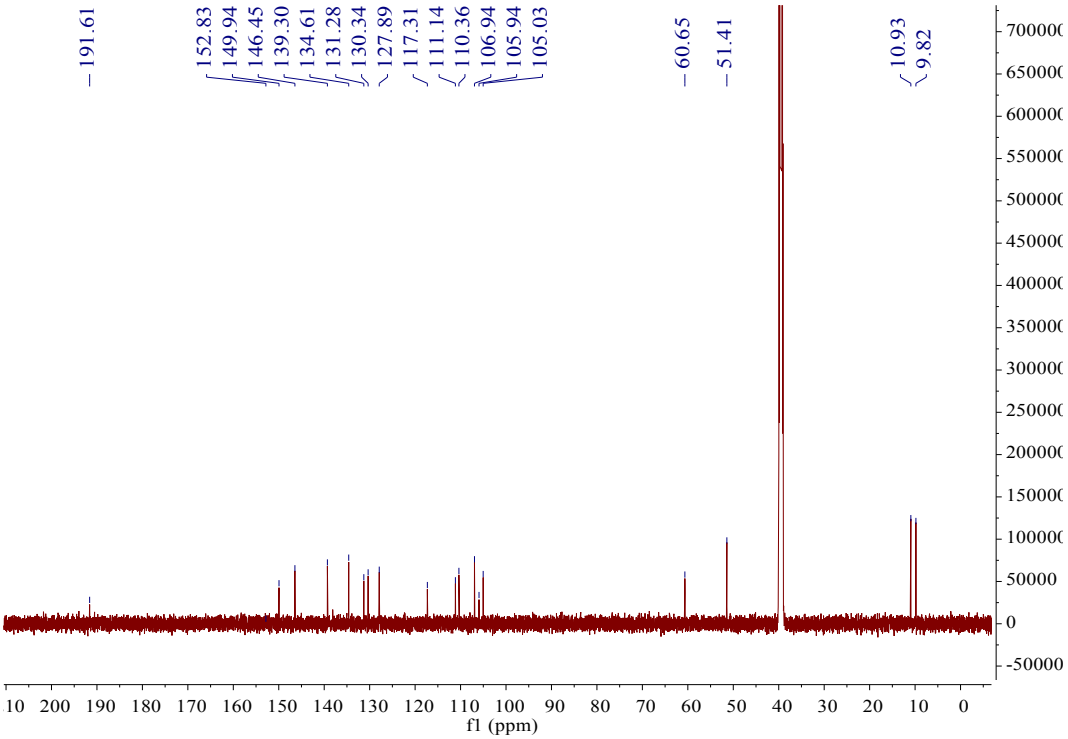

Fig. S35 ^{13}C NMR (150 MHz, DMSO-d_6) spectra of **4a**/**4b**

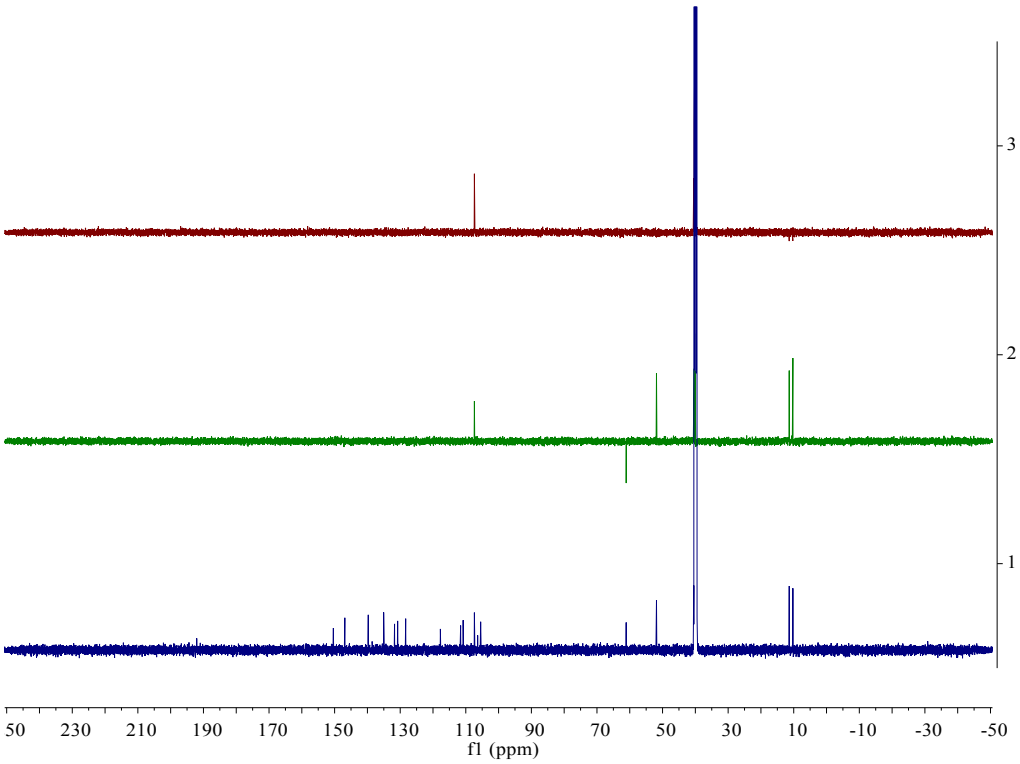

Fig. S36 DEPT NMR (150 MHz, DMSO-d_6) spectra of **4a**/**4b**

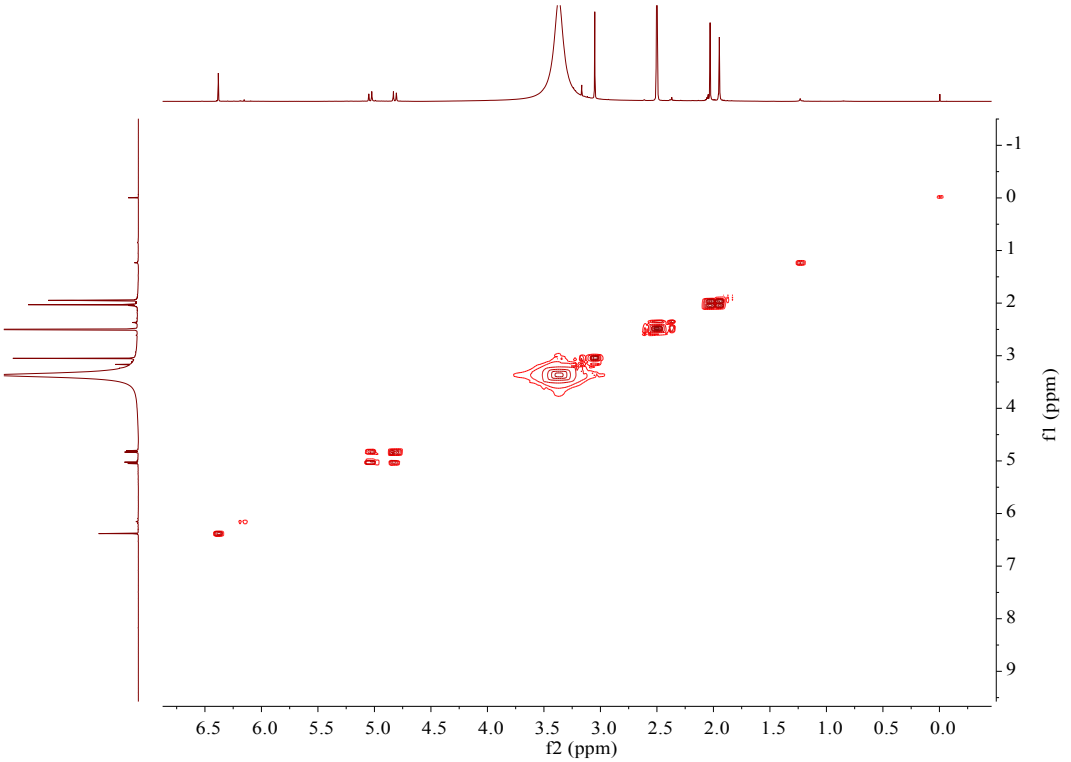

Fig. S37 ^{1}H-^{1}H COSY NMR (600 MHz, DMSO-d_6) spectra of **4a**/**4b**

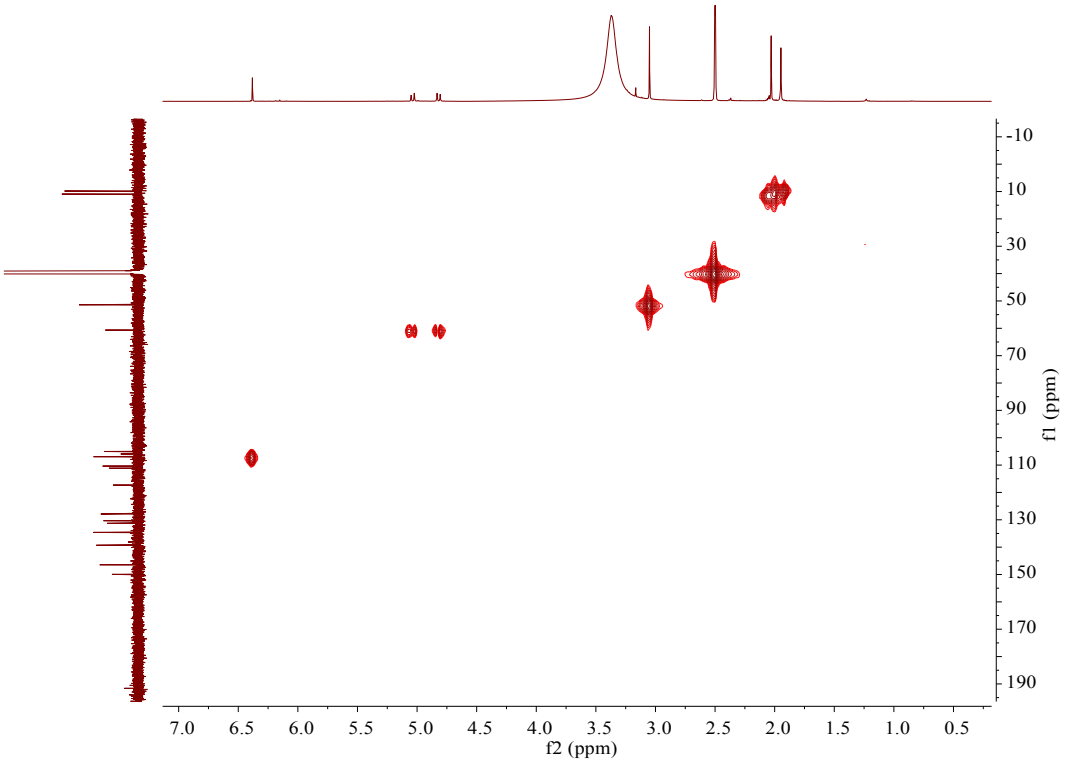

Fig. S38 HSQC NMR (600 MHz, DMSO-d_6) spectra of **4a**/**4b**

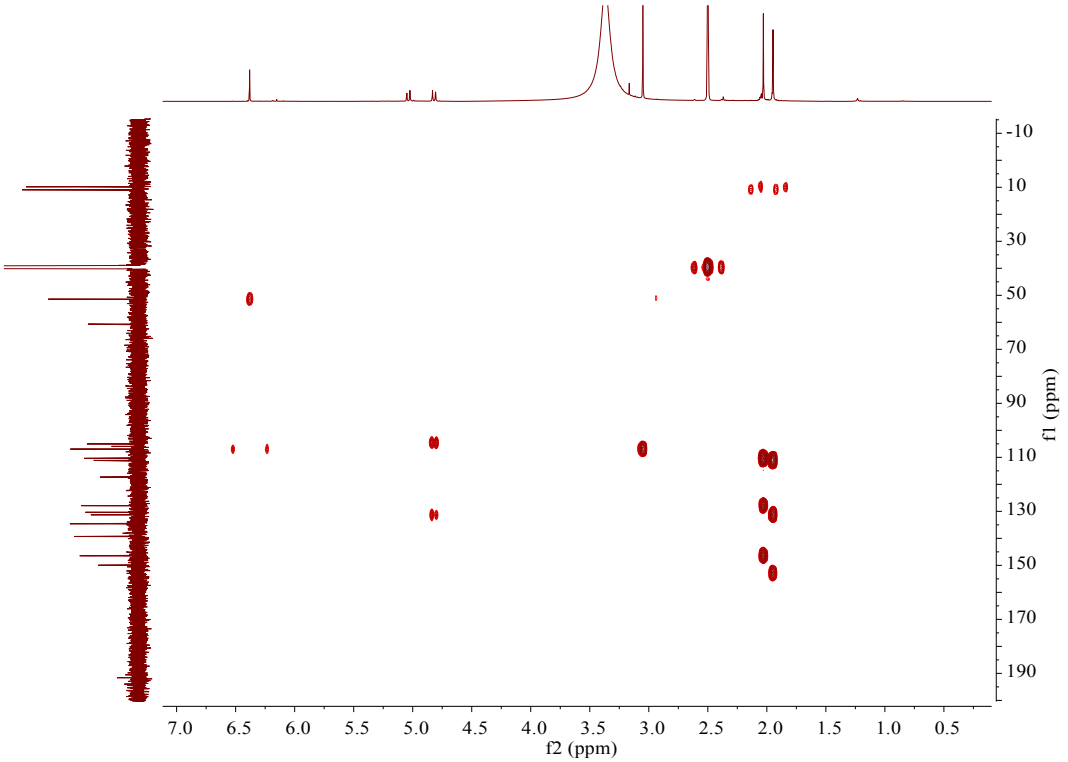

Fig. S39 HMBC NMR (600 MHz, DMSO-d_6) spectra of **4a**/**4b**

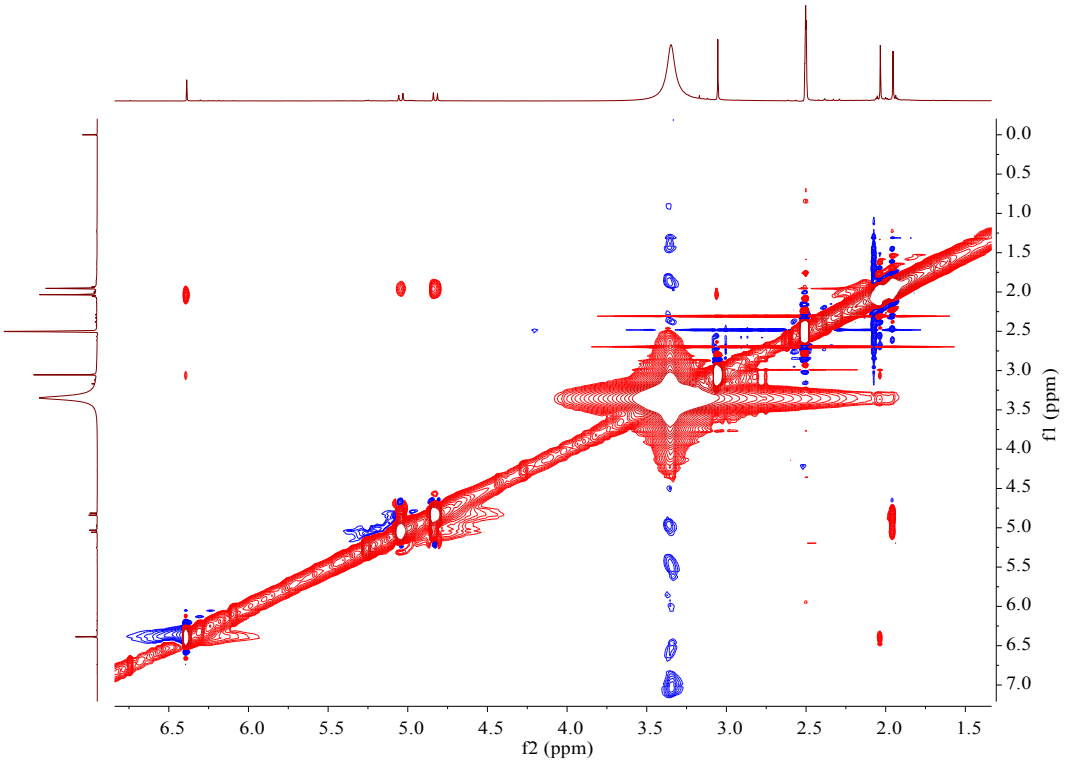

Fig. S40 NOESY NMR (600 MHz, DMSO-d_6) spectra of **4a**/**4b**

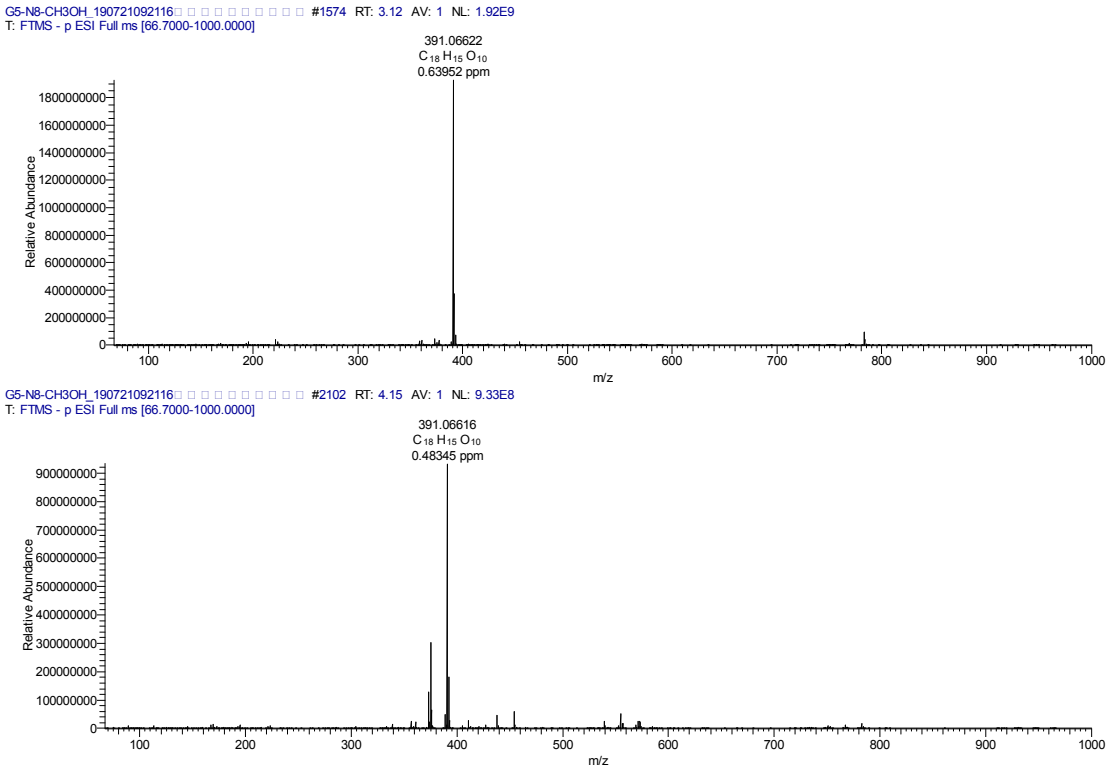

Fig. S41 HR-ESI-MS spectrum of **5** and **6**

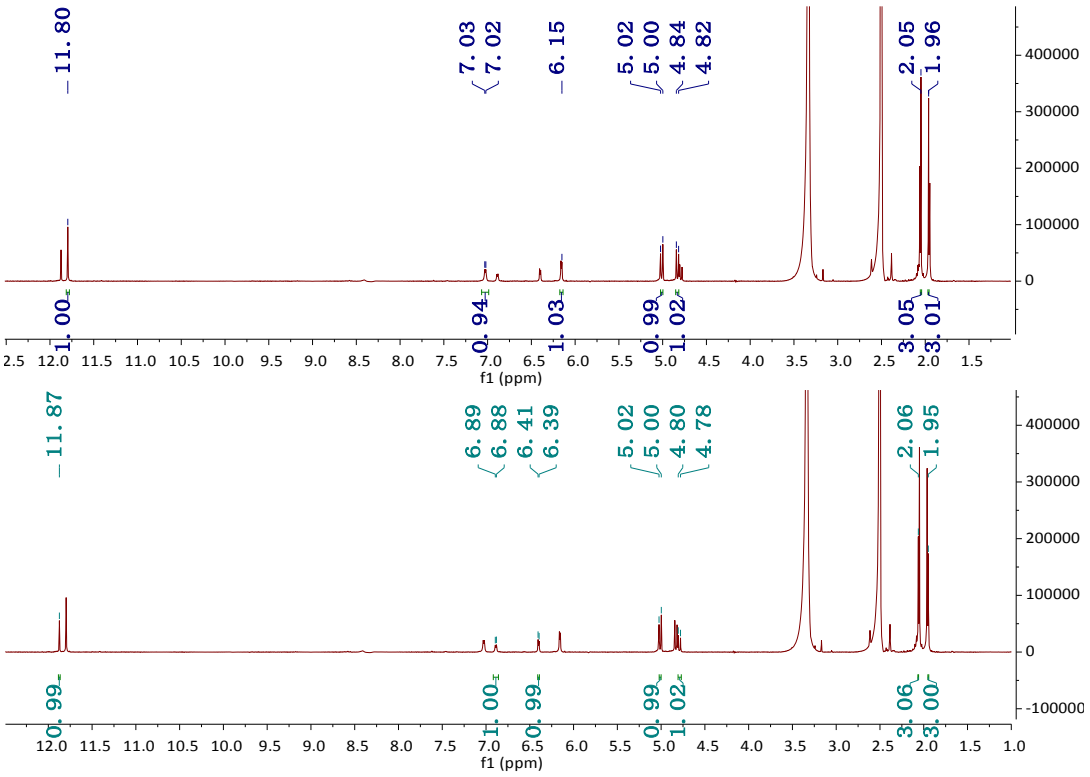

Fig. S42 ^{1}H NMR (600 MHz, DMSO-d_6) spectra of **5** and **6**

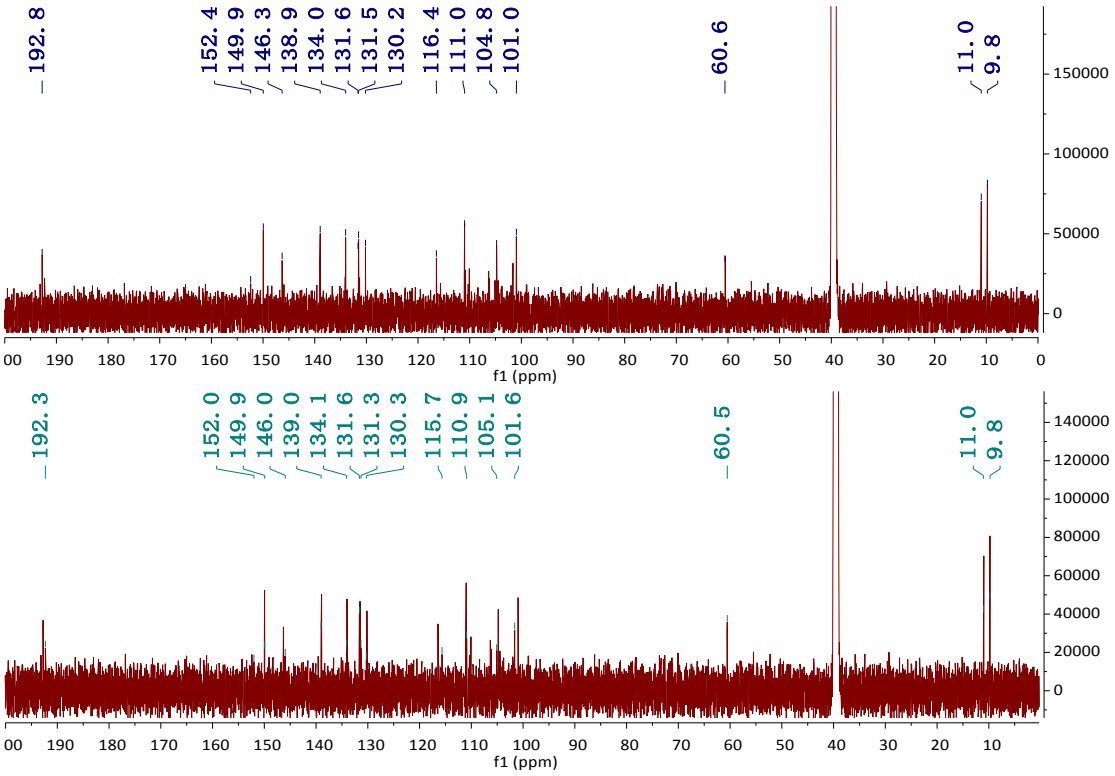

Fig. S43 ^{13}C NMR (150 MHz, DMSO-d_6) spectra of **5** and **6**

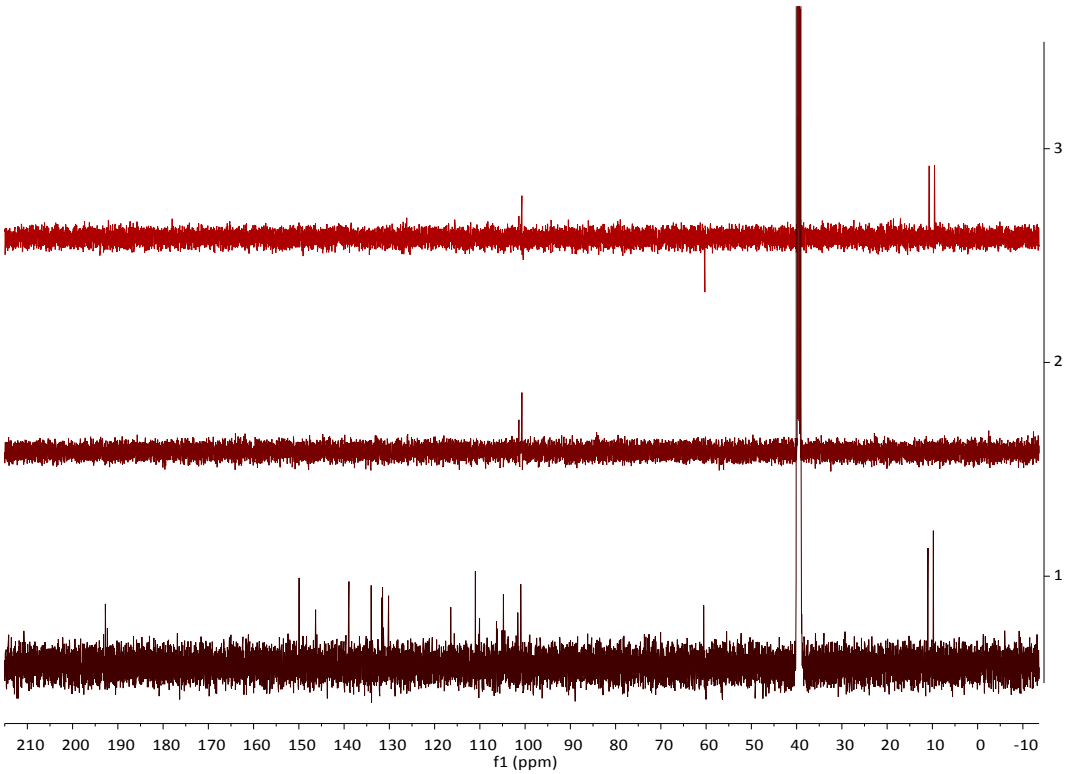

Fig. S44 DEPT NMR (150 MHz, DMSO-d_6) spectra of **5** and **6**

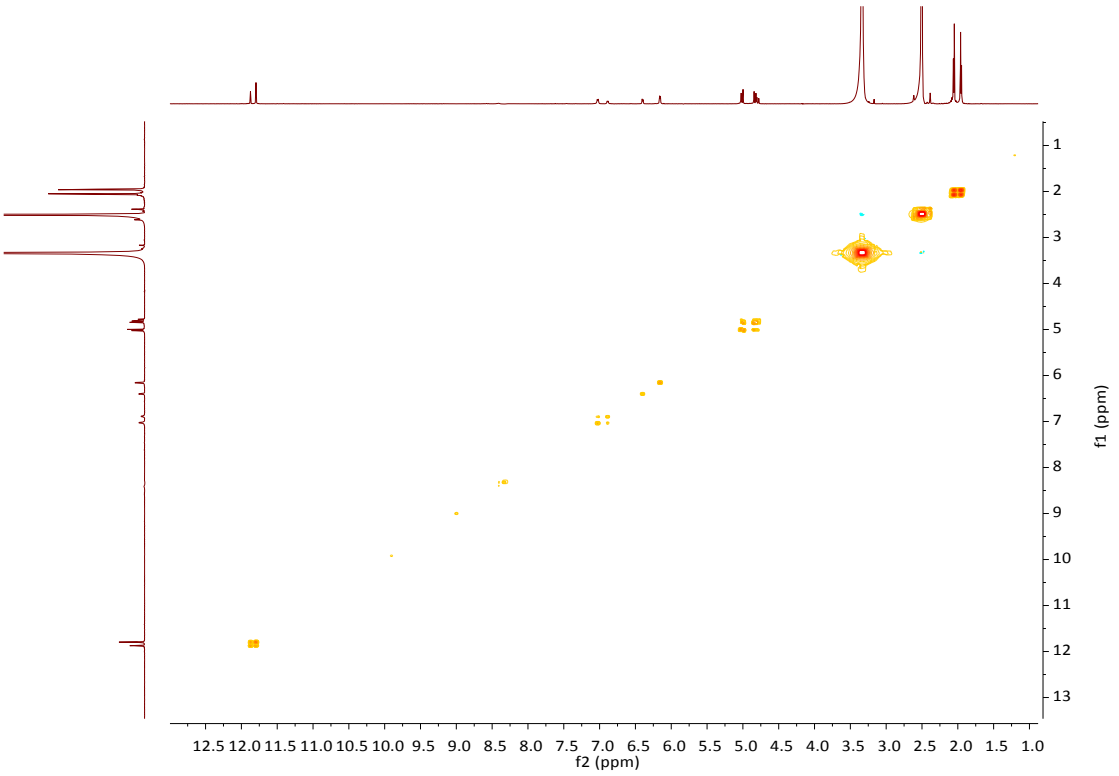

Fig. S45 ^{1}H-^{1}H COSY NMR (600 MHz, DMSO-d_6) spectra of **5** and **6**

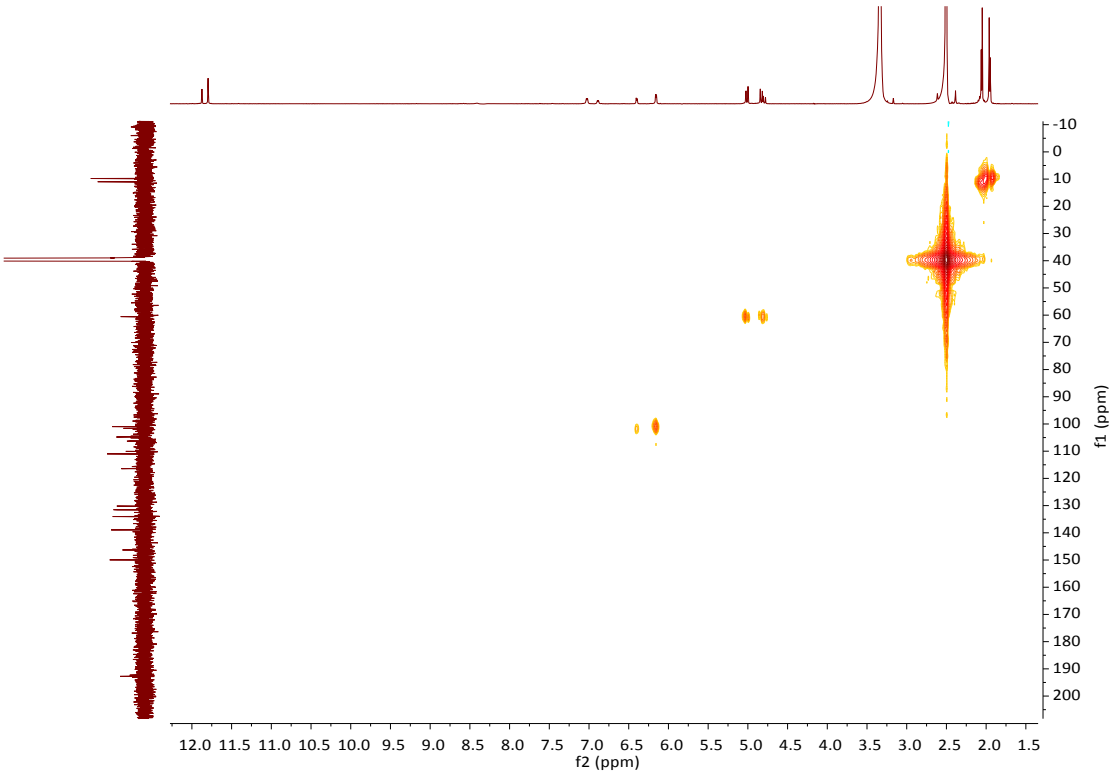

Fig. S46 HSQC NMR (600 MHz, DMSO-d_6) spectra of **5** and **6**

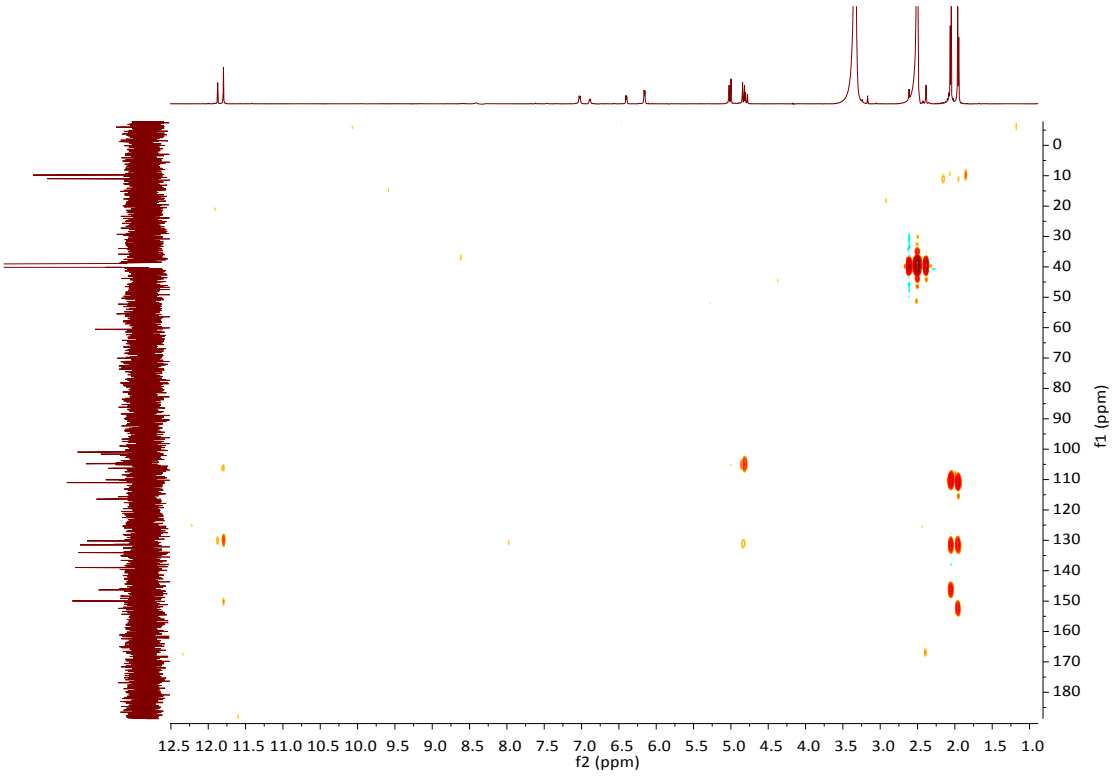

Fig. S47 HMBC NMR (600 MHz, DMSO-d_6) spectra of **5** and **6**

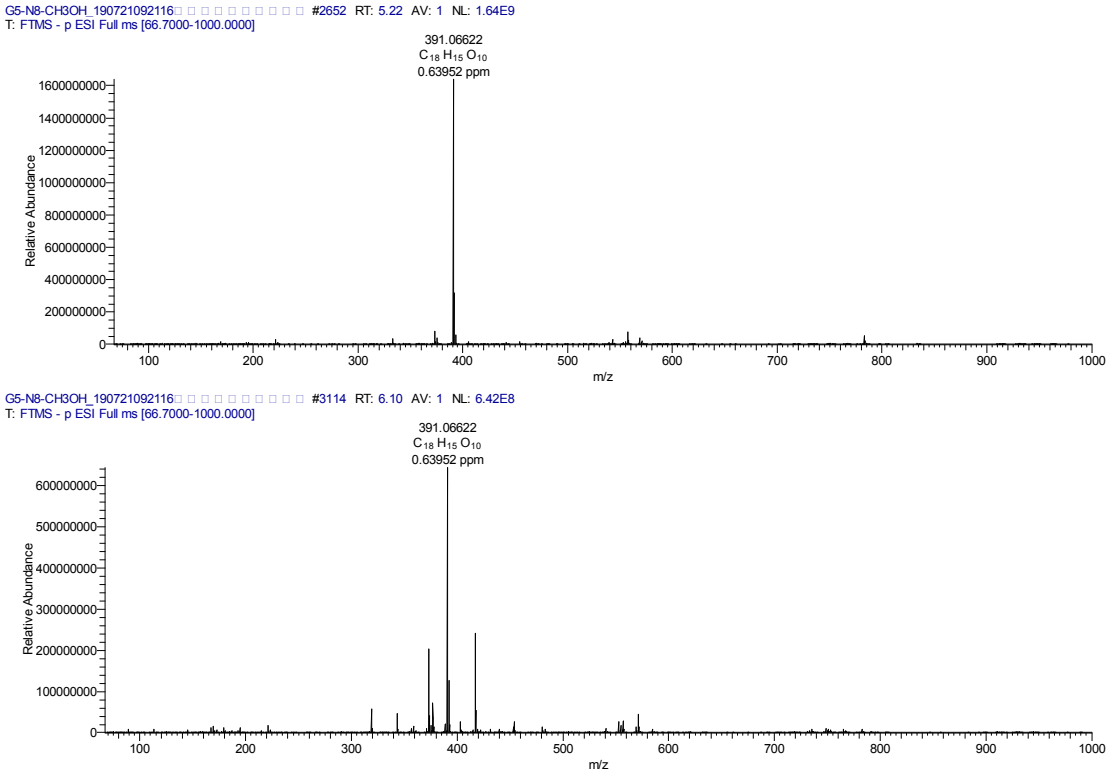

Fig. S48 HR-ESI-MS spectrum of **7** and **8**

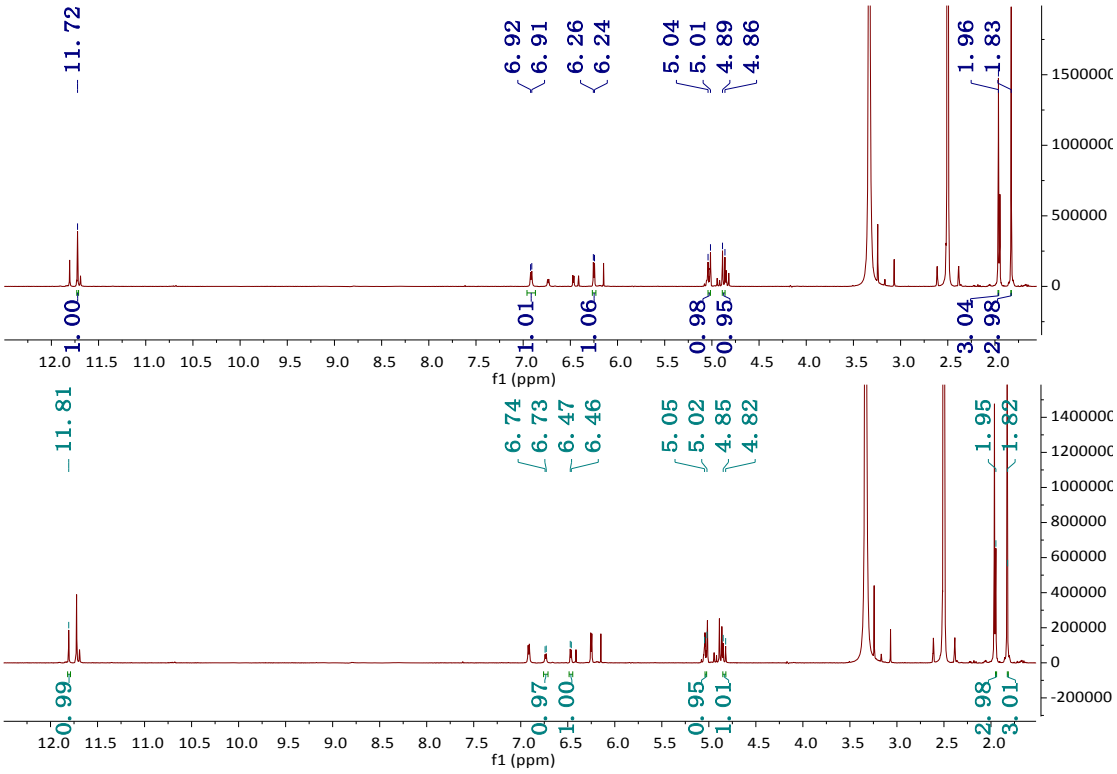

Fig. S49 ^{1}H NMR (600 MHz, DMSO-d_6) spectra of **7** and **8**

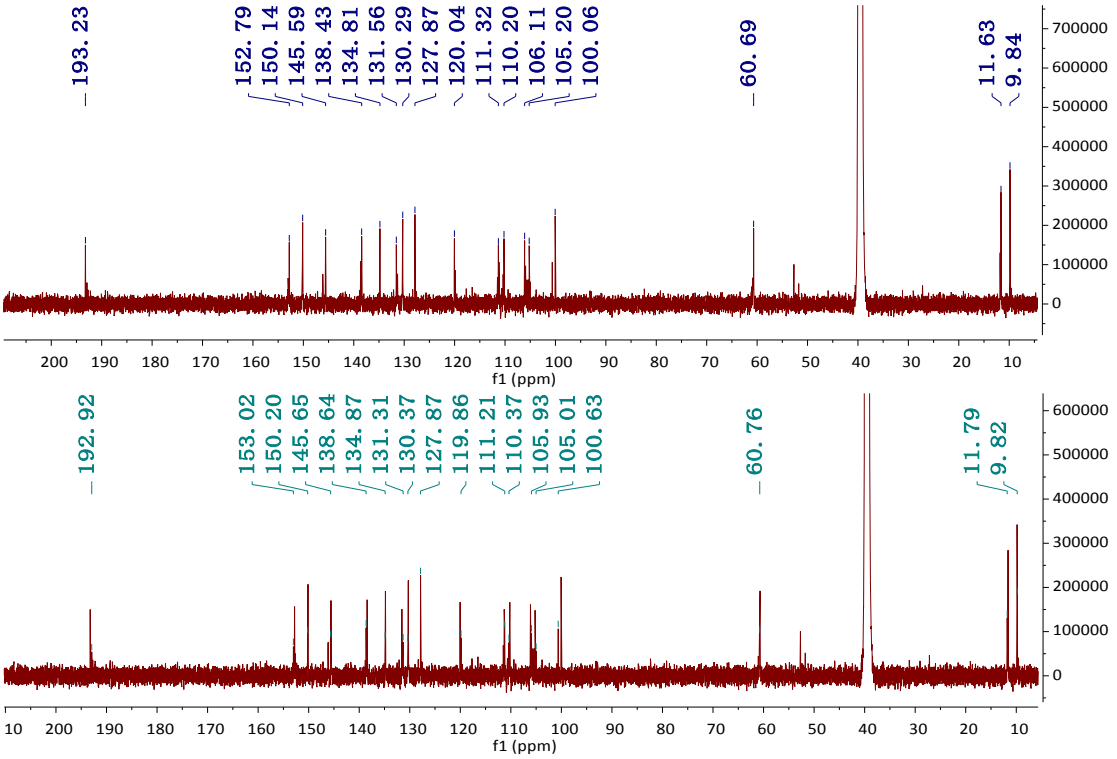

Fig. S50 ^{13}C NMR (150 MHz, DMSO-d_6) spectra of **7** and **8**

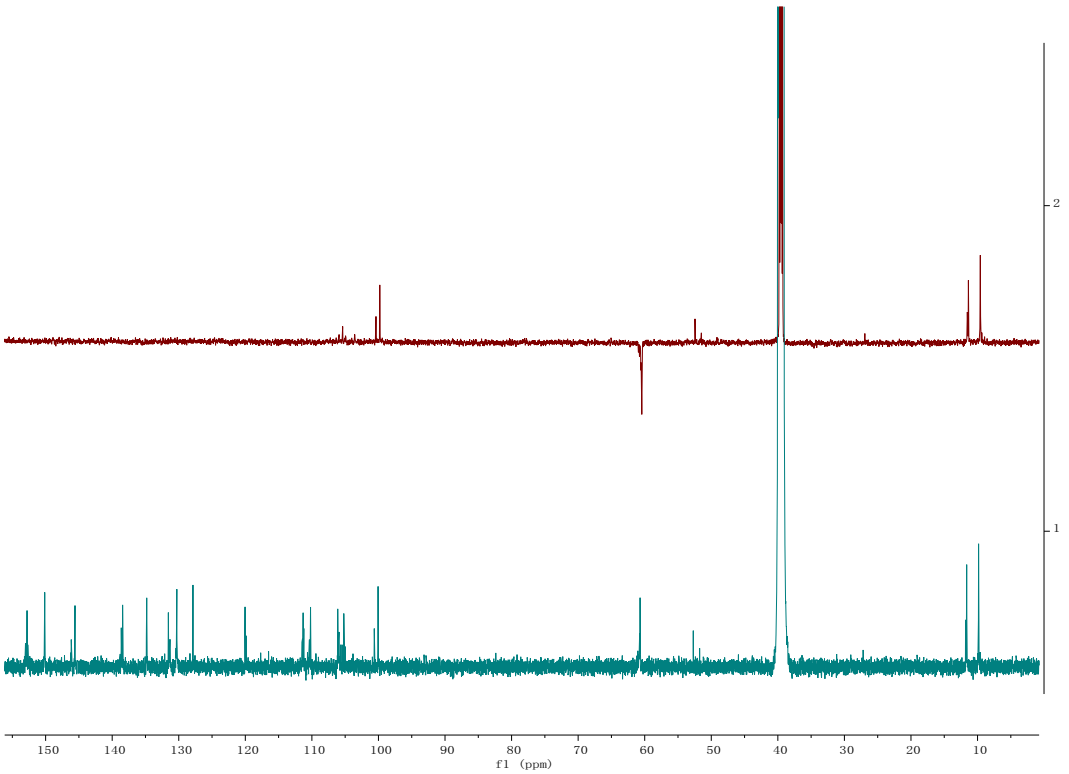

Fig. S51 DEPT-135 NMR (150 MHz, DMSO-d_6) spectra of **7** and **8**

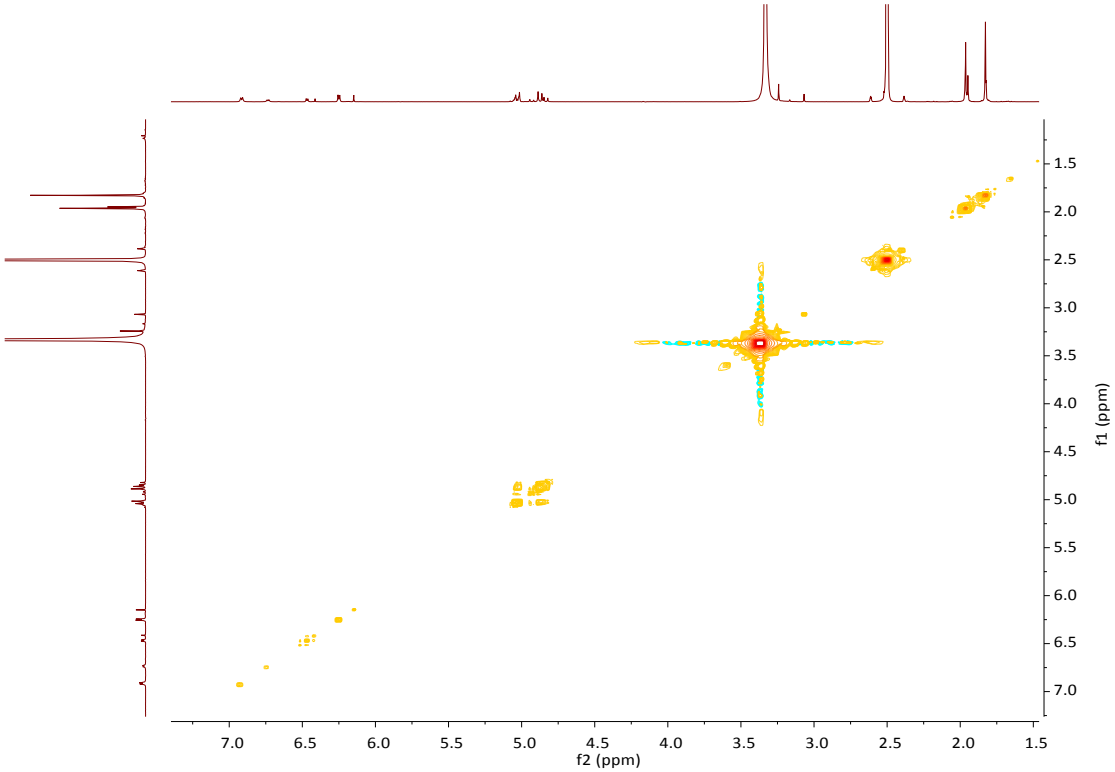

Fig. S52 DEPT-135 NMR (150 MHz, DMSO-d_6) spectra of **7** and **8**

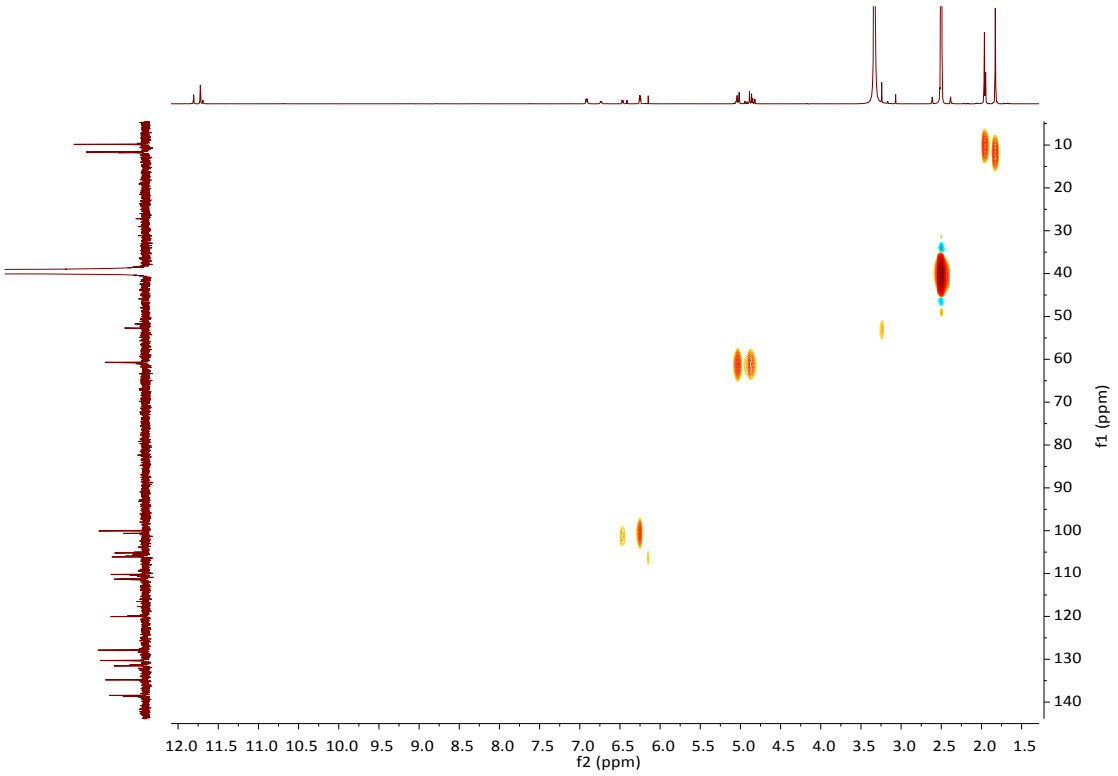

Fig. S53 HSQC NMR (600 MHz, DMSO-d_6) spectra of **7** and **8**

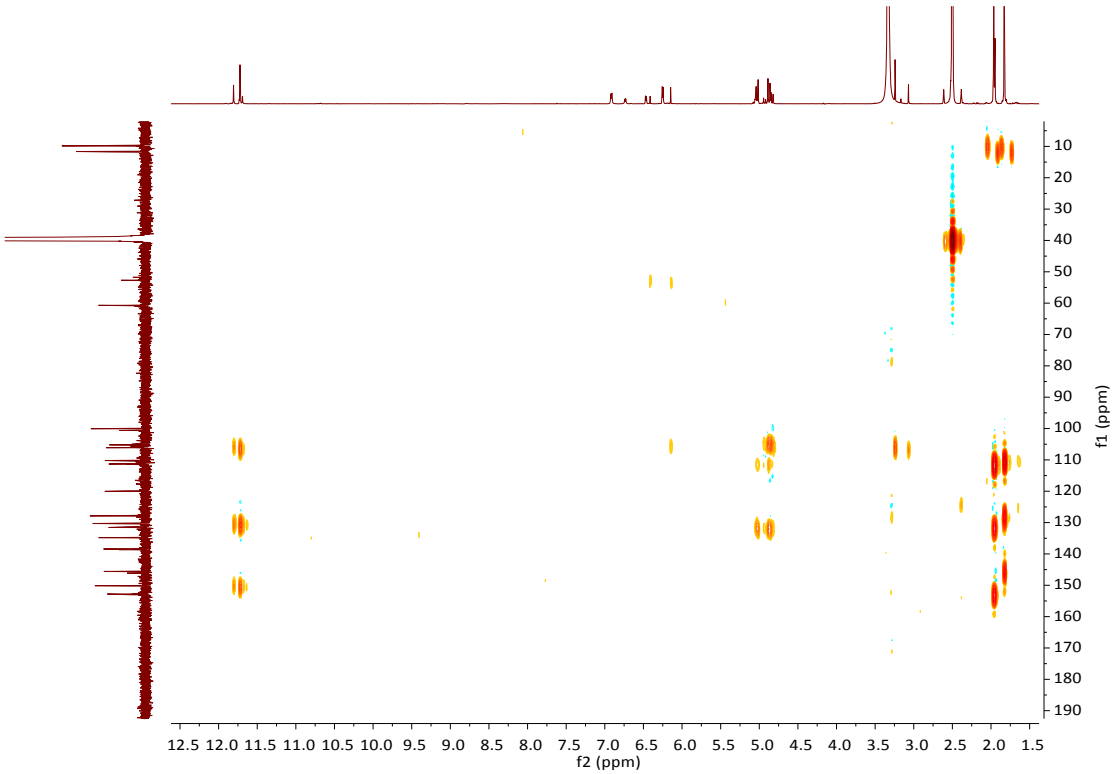

Fig. S54 HMBC NMR (600 MHz, DMSO-d_6) spectra of **7** and **8**

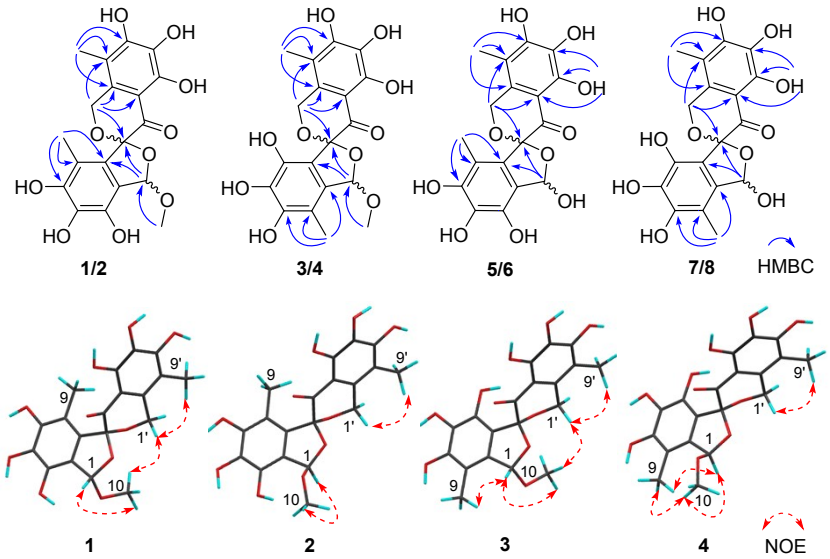

Fig. S55 Key HMBC correlations of **1**−**8** and Key NOE correlations of **1**−**4**

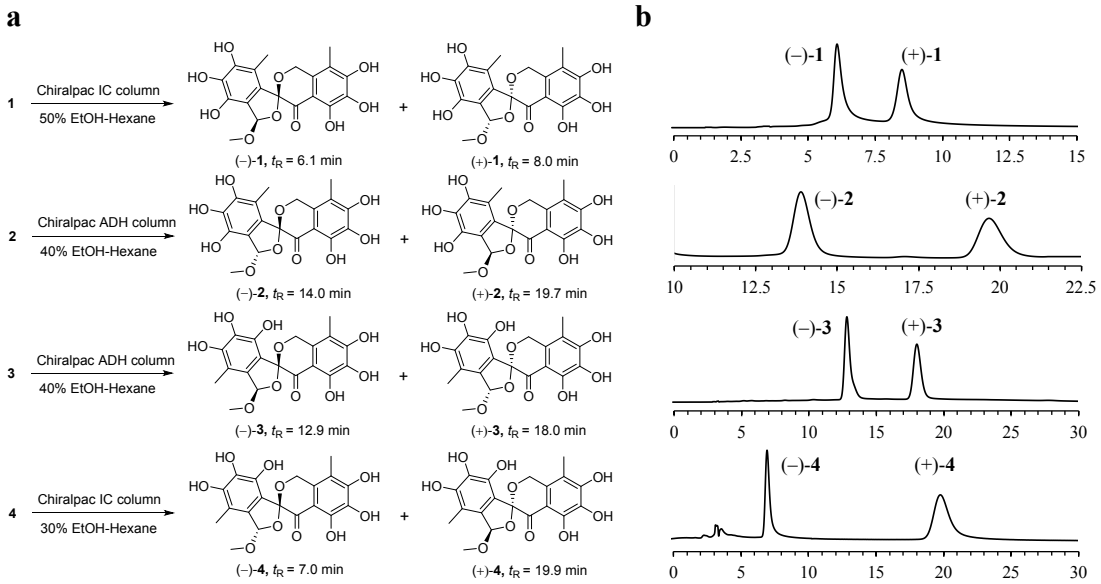

Fig. S56 Chiral seperation of compounds **1**–**4.** (**a**) Conditions for chiral seperation of **1**−**4**; (**b**) HPLC chromatograms of **1**–**4** running with a chiral column (DAD, λ = 300 nm)

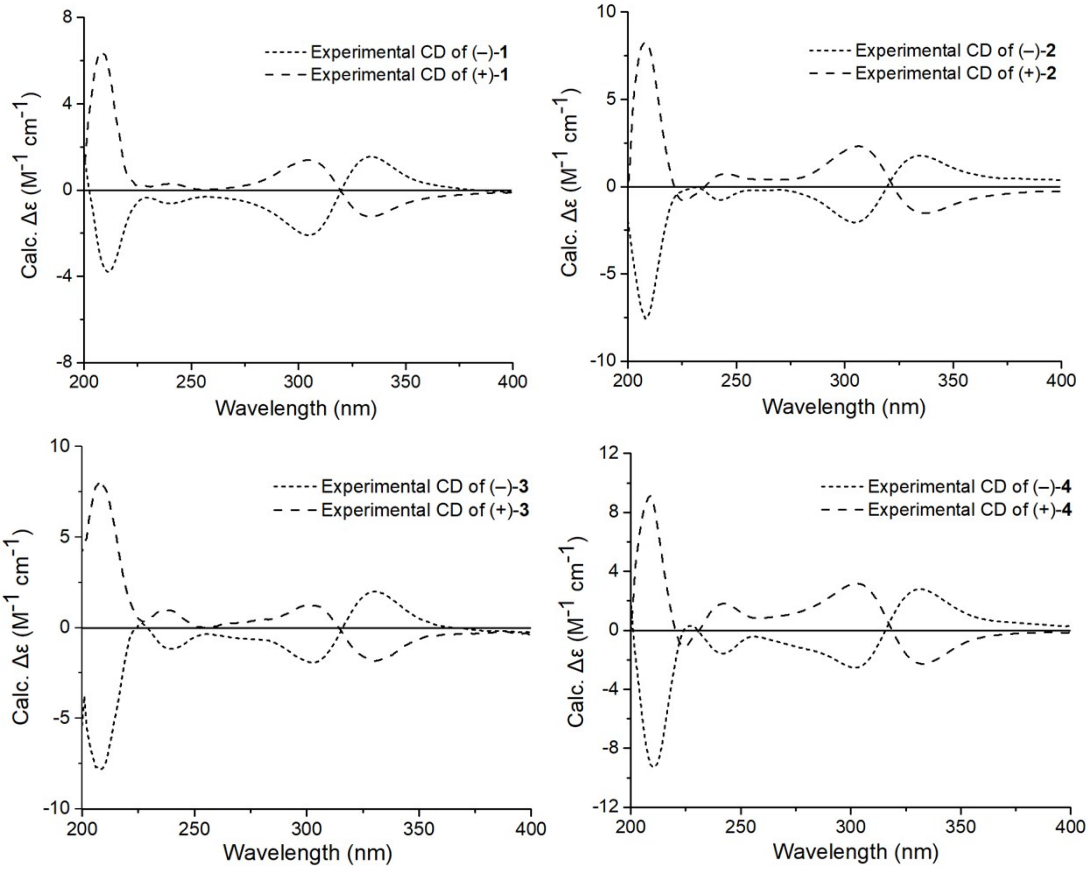

Fig. S57 Experimental CD of compounds **1**–**4**

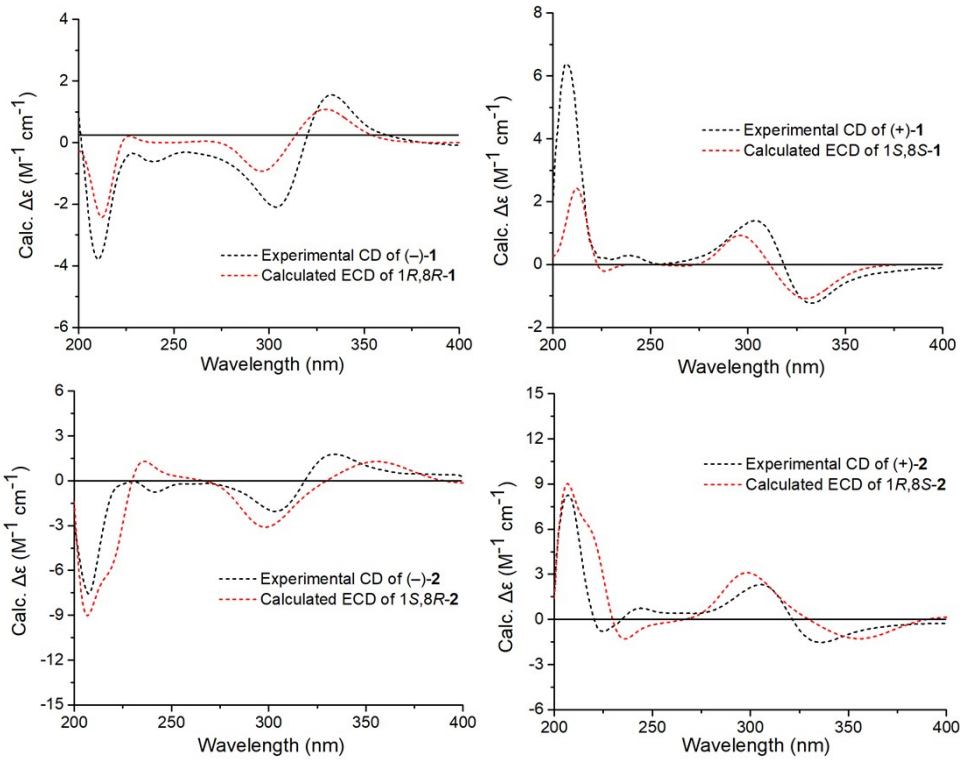

Fig. S58 Computed ECD of compounds (±)-**1** and (±)-**2**

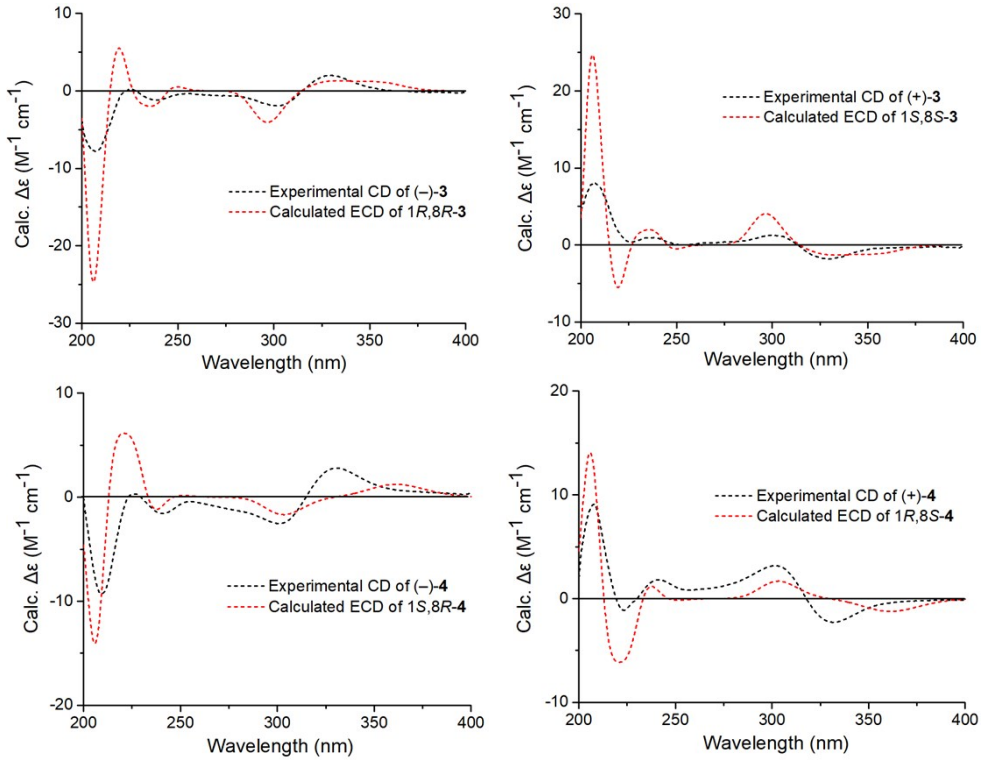

Fig. S59 Computed ECD of compounds (±)-**3** and (±)-**4**

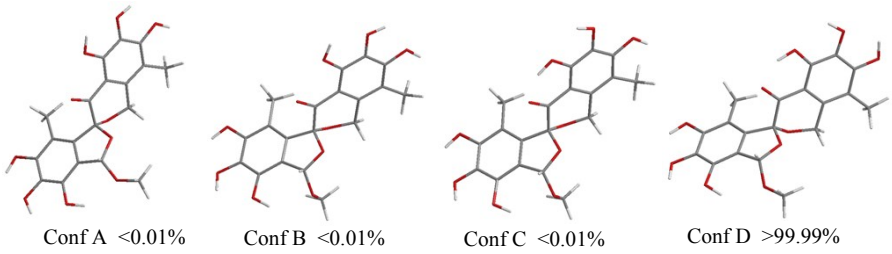

Fig. S60 DFT-optimized structures for low-energy conformers of 1*S*,8*S*-**1** at B3LYP/6-31G(d) level in methanol (PCM).

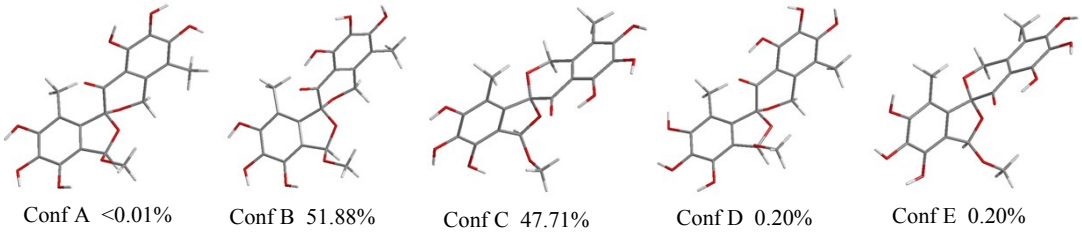

Fig. S61 DFT-optimized structures for low-energy conformers of 1*R*,8*S*-**2** at B3LYP/6-31G(d) level in methanol (PCM).

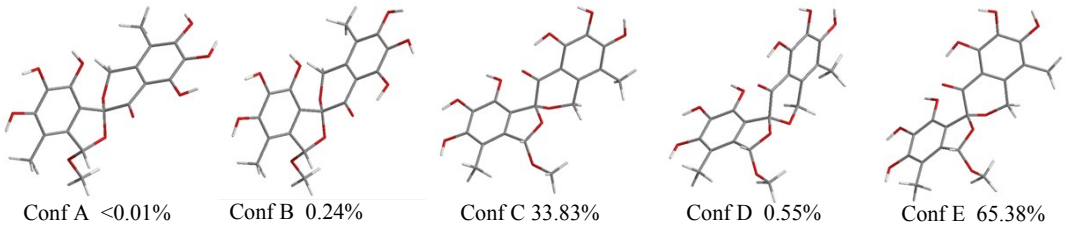

Fig. S62 DFT-optimized structures for low-energy conformers of 1*S*,8*S*-**3** at B3LYP/6-31G(d) level in methanol (PCM).

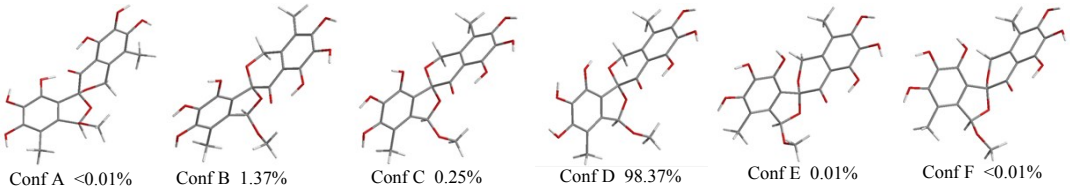

Fig. S63 DFT-optimized structures for low-energy conformers of 1*R*,8*S*-**4** at B3LYP/6-31G(d) level in methanol (PCM).

Supplementary Tables

Table. S1 Annotation for each node in the epicospirocin cluster (Clutser I in **Fig**. **S46**) of the EN09116 molecular networking.

Node	*m/z*	Annotation
1	258.026	-
2	295.091	-
3	331.084	$-O_2$ ($\Delta m/z$ = -32.026) from cpd.**9**/**11**
4	357.063	epicoccolide B $[M-H]^-$
5	359.031	$+H_2$ ($\Delta m/z$ = 1.968) from epicoccolide B
6	363.110	cpd.**9** or cpd.**11** $[2M-H]^-$
7	373.065	epicoccolide A $[M-H]^-$
8	375.077	eleganketal A $[M-H]^-$
9	377.089	flavimycin A $[M-H]^-$
10	378.093	isotopic peak for flavimycin A ($\Delta m/z$ = 1.004)
11	387.088	$+CH_2$ ($\Delta m/z$ = 14.023) from epicoccolide A
12	389.093	$+CH_2$ ($\Delta m/z$ = 14.016) from eleganketal A
13	391.067	epicospirocin B, 1-*epi*-epicospirocin B, epicospirocin C, 1-*epi*-epicospirocin C, cpd.**15** or cpd.**17** $[M-H]^-$
14	393.083	cpd.**14** or cpd.**16** $[M-H]^-$
15	405.082	(±)-epicospirocin A, (±)-1-epi-epicospirocin A, (±)-aspermicrone B, (±)-aspermicrone C, $[M-H]^-$
16	413.066	$+C_3H_4O$ ($\Delta m/z$ = 56.003) from epicoccolide B
17	417.146	$+C_2H_2O$ ($\Delta m/z$ = 42.069) from eleganketal A
18	422.074	+HO ($\Delta m/z$ = 16.992) from (±)-epicospirocin A
19	429.061	$+H_4O_2$ ($\Delta m/z$ = 35.978) from cpd.**14**/**16**
20	431.31	$+C_2H_2$ ($\Delta m/z$ = 26.228) from (±)-epicospirocin A
21	438.069	$+HO_2$ ($\Delta m/z$ = 32.987) from (±)-epicospirocin A
22	440.085	$+H_3O_2$ ($\Delta m/z$ = 35.003) from (±)-epicospirocin A
23	454.101	-
24	458.08	-
25	470.147	-
26	492.435	-
27	539.122	-
28	553.101	-
29	555.116	-
30	557.132	-
31	559.111	-
32	561.31	-
33	570.182	-
34	573.127	-

35	585.127	-
36	602.117	-
37	618.112	-
38	620.128	-
39	636.123	
40	719.165	-
41	735.169	-
42	751.154	eleganketal A $[2M-H]^-$
43	765.17	-
44	1165.4	-

"-" means less possible to be dibenzospiroketal anologs.

Table. S2 Antibacterial activity of compounds **1**–**8**

Compound	Pathogenic bacteria (MIC, μg/mL)				
	C. albicans	*S. aureus*	MRSA	*S. mutans*	*S. sanguis*
1	64	64	64	>64	>64
2	64	64	64	>64	>64
3	64	>64	>64	>64	>64
4	64	64	64	>64	>64
5 + 6	>64	>64	64	>64	>64
7 + 8	>64	64	64	>64	>64
Control	1[a]	1[b]	1[b]	2[b]	1[b]

[a]Amphotericin B, [b]Vancomycin

Table. S3 Deduced functions of orfs in the putative epispirokicin gene cluster (1819)

ORF	Size	Proposed function	origin (protein ID); Identity/Similarity (%)
esp1	157	aliphatic nitrilase	*Periconia macrospinosa* (PYI11620.1); 41.1/50.7
esp2	198	helix-turn-helix-domain containing protein type	*Stemphylium lycopersici* (KNG46860.1); 56.9/71.8
esp3	2594	polyketide synthase	*Aspergillus sclerotioniger* CBS 115572 (XP_025464304.1);41.9/59.0
esp4	1036	NRPS-like enzyme	*Aspergillus sclerotioniger* CBS 115572 (XP_025464317.1); 43.5/60.1
esp5	217	hypothetical protein B5807_11146	*Epicoccum nigrum* (OSS44045.1); 100/100
esp6	739	Phenol hydroxylase	*Cutaneotrichosporon cutaneum* (P15245.3); 27.8/41.5
esp7	510	Cytochrome P450 monooxygenase pkfB	*Aspergillus nidulans FGSC A4* (C8VI81.1); 45.0/59.3
esp8	433	MFS general substrate transporter	*Aspergillus ibericus* CBS 121593 (XP_025573314.1); 52.0/67.8

Table. S4 Mass difference, observed and calculated *m/z* value of each biosynthetic precursor presented in the EN09116 MS/MS-molecular networking.

Compound	Molecular formula	Calculated *m/z*	Observed *m/z*	[a]Δ (ppm)
9	$C_9H_9O_4$ [M-H]$^-$	181.0506	181.0505	0.55
	$C_{18}H_{19}O_8$ [2M-H]$^-$	363.1080	363.1098	4.96
10	$C_9H_9O_3$ [M-H]$^-$	165.0557	165.0554	1.82
11	$C_9H_9O_4$ [M-H]$^-$	181.0506	181.0505	0.55
12	$C_9H_9O_5$ [M-H]$^-$	197.0456	197.0456	0.36
13	$C_9H_7O_5$ [M-H]$^-$	195.0299	195.0299	0.05
14	$C_{18}H_{17}O_{10}$ [M-H]$^-$	393.0842	393.0827	3.81
15	$C_{18}H_{15}O_{10}$ [M-H]$^-$	391.0663	391.0671	2.04
16	$C_{18}H_{17}O_{10}$ [M-H]$^-$	393.0842	393.0827	3.81
17	$C_{18}H_{15}O_{10}$ [M-H]$^-$	391.0663	391.0671	2.04

[a]Δ = Observed *m/z* − Calculated *m/z*

Table. S5 Primers used in this study

Primer	Sequence (5' to 3')
Esp3-up-F	TATGTCTGGAGGTGGGGTGG
Esp3-up-R	TCAATATCATCTTCTGTCGATTTGCAATTGGTTCAAAAGG
Esp3-dn-F	GTTTAGAGGTAATCCTTCTTGCACATGGAACAGGTACACC
Esp3-dn-R	GAACCAACGACCACATGACT
Esp3-F	GAAACGTCGGGGGGTTCTTG
Esp3-R	AATAGCAAGCATTGCGCCTC
hph-F	TCGACAGAAGATGATATTGA
hph-R	AAGAAGGATTACCTCTAAAC
Esp4-up-F	TCACCAAATTTGAAGCCTTTC
Esp4-up-R	TCAATATCATCTTCTGTCGAGGTCTTGATCCGATGTTTAGA
Esp4-dn-F	GTTTAGAGGTAATCCTTCTTACTGTAAAGTCTCCGTTCAC
Esp4-dn-R	CCAGAAAGAATCCAGATCCT
Esp4-F	ACCAGTGAAGGTGGAGTAAA
Esp4-R	CCCTCAAGTGCCACTTCCTA

Table. S6 List of 55 NR-PKSs related to known polyketides

S/N	Group	Cyclization	Accession No.	Strain	Products
1	I	C2-C7	XP_681178	*Aspergillus nidulans* FGSC A4	Orsellinic acid
2	I	C2-C7	ACM42403	*Chaetomium chiversii*	Radicicol
3	I	C2-C7	ABB90282	*Fusarium graminearum*	Zearalenone
4	I	C2-C7	ACD39762	*Hypomyces subiculosus*	Hypocemycin
5	I	C2-C7	ACD39770	*Metacordyceps chlamydosporia*	Radicicol
6	I	C3-C8	AGC95321	*Aspergillus terreus*	10,11-

					Dehydrocurvularin
7	II	C2-C7	BAD22832	*Bipolaris oryzae*	THN
8	II	C2-C7	AAO60166	*Ceratocystis resinifera*	THN
9	II	C2-C7	BAA18956	*Colletotrichum lagenaria*	THN
10	II	C2-C7	ABU63483	*Elsinoe fawcettii*	Elsinochrome
11	II	C2-C7	AAD31436	*Exophiala dermatitidis*	THN
12	II	C2-C7	AAN75188	*Exophiala lecanii-corni*	THN
13	II	C2-C7	AAN59953	*Glarea lozoyensis*	THN
14	II	C2-C7	AAD38786	*Nodulisporium* sp.ATCC74245	THN
15	II	C2-C7	ABD47522	*Ophiostoma piceae*	THN
16	II	C2-C7	CAM35471	*Sordaria macrospora*	THN
17	III	C2-C7	AAC39471	*Aspergillus fumigatus*	Naphthopyrones
18	III	C2-C7	EDP55264	*Aspergillus fumigatus* A1163	THN
19	III	C2-C7	Q03149	*Aspergillus nidulans* FGSC A4	YWA1, Naphthopyrone
20	III	C2-C7	EHA28527	*Aspergillus niger* ATCC 1015	YWA1, dimeric naphtho-γ-pyrones
21	III	C2-C7	CAB92399	*Fusarium fujikuroi*	Bikaverin
22	III	C2-C7	AAU10633	*Fusarium graminearum*	Aurofusarin
23	IV	C4-C9	AAA81586	*Aspergillus nidulans*	sterigmatocystin
24	IV	C4-C9	Q12397	*Aspergillus nidulans* FGSC A4	sterigmatocystin
25	IV	C4-C9	ACH72912	*Aspergillus ochraceoroseus*	Aflatoxin
26	IV	C4-C9	BAE71314	*Aspergillus oryzae*	Aflatoxin
27	IV	C4-C9	Q12053	*Aspergillus parasiticus*	Aflatoxin
28	IV	C4-C9	AAT69682	*Cercospora nicotianae*	THN
29	IV	C4-C9	CCE67070	*Fusarium fujikuroi*	Fusarubin
30	IV	C4-C9	AAS92537	*Leptosphaeria maculans*	Sirodesmin
31	IV	C4-C9	AAZ95017	*Mycosphaerella pini*	Aflatoxin
32	IV	C4-C9	XP_003039929	*Nectria haematococca*	Bostrycoidin,fusarubin
33	V	C1-C6	ADI24953	*Penicillium aethiopicum*	griseofulvin
34	V	C2-C7	XP_664675	*Aspergillus nidulans* FGSC A4	dehydrocitreoisocoumarin, citreisocoumarin, alternariol
35	V	C6-C11	XP_746435	*Aspergillus fumigatus* Af293	Endocrocin
36	V	C6-C11	XP_657754	*Aspergillus nidulans* FGSC A4	Atrochrysone carboxylic acid
37	V	C6-C11	XP_663604	*Aspergillus nidulans* FGSC A4	Asperthecin
38	V	C6-C11	XP_001394705	*Aspergillus niger* CBS 513.88	TAN-1612, BMS-192548
39	V	C6-C11	XP_001217072	*Aspergillus terreus* NIH2624	Emodin
40	V	C6-C11	ADI24926	*Penicillium aethiopicum*	viridicatumtoxin

41	VI	C2-C7	XP_681652	*Aspergillus nidulans* FGSC A4	3,5-dimethylorsellinic acid, austinol,dehydroaustinol
42	VI	C2-C7	ADY00130	*Penicillium brevicompactum*	5-methylorsellinic acid, mycophenolic acid
43	VI	C2-C7	XP_664052	*Aspergillus nidulans* FGSC A4	3-methylorsellinic acid, cichorine
44	VII	C2-C7	XP_658638	*Aspergillus nidulans* FGSC A4	asperfuranone
45	VII	C2-C7	XP_660990	*Aspergillus nidulans* FGSC A4	2,4-dihydroxy-3-methyl-6-(2-oxoundecyl)benzaldehyde
46	VII	C2-C7	XP_658127	*Aspergillus nidulans* FGSC A4	2-ethyl-4,6-dihydroxy-3,5-dimethylbenzaldehyde
47	VII	C2-C7	XP_660834	*Aspergillus nidulans* FGSC A4	orsellinaldehyde
48	VII	C2-C7	EHA28237	*Aspergillus niger* ATCC 1015	Azanigerone A
49	VII	C2-C7	AGN71604	*Monascus pilosus*	Rubropunctatin
50	VII	C2-C7	BAD44749	*Monascus purpureus*	citrinin
51	VII	C2-C7	CAN87161	*Sarocladium strictum*	3-methylorcinaldehyde
52	VII	C2-C7	XP_659636	*Aspergillus nidulans* FGSC A4	2,4-dihydroxy-6-[(3E,5E,7E)-2-oxonona-3,5,7-trienyl]benzaldehyde
53	VII	C2-C7	XP_001212610	*Aspergillus terreus* NIH2624	citrinin
54	VII	C2-C7	ANID_07903	*Aspergillus nidulans* FGSC A4	2,4-dihydroxy-3-methyl-6-(2-oxopropyl)benzaldehyde
55	VIII	C2-C7	AFL91703	*Armillaria mellea*	Orsellinic acid

Table. S7 ^{1}H (600 MHz) and ^{13}C (150 MHz) NMR data of **1**−**4** in DMSO-d_6

Pos.	**1**		**2**		**3**		**4**	
	δ_H[a] mult	δ_C[b]	δ_H[a] mult	δ_C[b]	δ_H[a] mult	δ_C[b]	δ_H[a] mult	δ_C[b]

	(*J* in Hz)		(*J* in Hz)		(*J* in Hz)		(*J* in Hz)	
1	6.15, s	105.6, CH	6.41, s	106.6, CH	6.10, s	106.4, CH	6.38, s	106.9, CH
2		116.5, C		116.5, C		128.2, C		127.9, C
3		138.6, C		139.2, C		110.3, C		110.4, C
4		134.8, C		135.2, C		146.4, C		146.4, C
5		146.1, C		146.7, C		134.6, C		134.6, C
6		110.4, C		111.1, C		139.1, C		139.3, C
7		128.4, C		129.1, C		117.0, C		117.3, C
8		105.8, C		106.0, C		105.0, C		105.0, C
9	1.82, s	11.6, CH_3	1.83, s	12.2, CH_3	2.02, s	10.9, CH_3	2.03, s	10.9, CH_3
10	3.24, s	52.7, CH_3	3.07, s	52.1, CH_3	3.24, s	52.4, CH_3	3.05, s	51.4, CH_3
1′	5.04, d (15.6); 4.93, d (15.6)	60.8, CH_2	5.06, d (15.7); 4.86, d (15.6)	61.2, CH_2	5.03, d (15.5); 4.88, d (15.4)	60.7, CH_2	5.04, d (15.5); 4.82, d (15.5)	60.7, CH_2
2′		131.3, C		131.7, C		131.3, C		131.3, C
3′		111.5, C		111.9, C		111.2, C		111.1, C
4′		153.6, C		153.6, C		152.9, C		152.8, C
5′		130.4, C		130.9, C		130.3, C		130.3, C
6′		150.1, C		150.4, C		149.9, C		149.9, C
7′		105.3, C		105.8, C		106.1, C		105.9, C
8′		192.5, C		192.4, C		192.2, C		191.6, C
9′	1.96, s	9.9, CH_3	1.95, s	10.3, CH_3	1.96, s	9.8, CH_3	1.95, s	9.8, CH_3

[a]Recorded at 600 MHz in DMSO-d_6. [b]Recorded at 125 MHz in DMSO-d_6.

Table. S8 ^{1}H (600 MHz) and ^{13}C (150 MHz) NMR data of **5**−**8** in DMSO-d_6

Pos.	**5** (or **6**)		**6** (or **5**)		**7** (or **8**)		**8** (or **7**)	
	δ_H[a] mult (*J* in Hz)	δ_C[b]	δ_H[a] mult (*J* in Hz)	δ_C[b]	δ_H[a] mult (*J* in Hz)	δ_C[b]	δ_H[a] mult (*J* in Hz)	δ_C[b]
1	7.02, d (6.8)	101.0, CH	6.89, d (7.2)	101.4, CH	6.91, d (7.3)	100.0, CH	6.73, d (7.4)	100.6, CH
1-OH	6.15, d (6.8)		6.40, d (7.2)		6.25, d (7.3)		6.46, d (7.4)	
2		130.2, C		130.3, C		127.9, C		127.9, C
3		110.1, C		110.3, C		110.2, C		110.4, C
4		146.3, C		146.0, C		146.0, C		145.7, C
5		134.0, C		134.1, C		134.8, C		134.9, C
6		138.9, C		139.0, C		138.4, C		138.6, C
7		116.4, C		115.7, C		120.0, C		119.9, C
8		104.8, C		105.1, C		105.2, C		105.0, C
9	2.05, s	11.0, CH_3	2.06, s	11.0, CH_3	1.83, s	11.6, CH_3	1.82, s	11.8, CH_3
1′	5.01, d (15.8);	60.6, CH_2	5.01, d (15.8);	60.5, CH_2	5.03, d (15.4);	60.7, CH_2	5.03, d (15.5);	60.8, CH_2

	4.83, d (15.8);		4.79, d (15.8);		4.87, d (15.4)		4.83, d (15.5)	
2′		131.6, C		131.6, C		131.6, C		131.3, C
3′		111.0, C		110.9, C		111.3, C		111.2, C
4′		152.4, C		152.0, C		152.8, C		153.0, C
5′		131.5, C		131.3, C		130.3, C		130.4, C
6′		149.9, C		149.9, C		150.1, C		150.2, C
6′-OH	11.80, s		11.87, s		11.72, s		12.81, s	
7′		106.3, C		106.2, C		106.1, C		105.9, C
8′		192.8, C		192.3, C		193.2, C		192.9, C
9′	1.96, s	9.8, CH_3	1.95, s	9.8, CH_3	1.96, s	9.8, CH_3	1.95, s	9.8, CH_3

[a]Recorded at 600 MHz in DMSO-d_6. [b]Recorded at 125 MHz in DMSO-d_6.

Reference

1. S. Haridas, C. Breuill, J. Bohlmann and T. Hsiang, *Journal of microbiological methods*, 2011, **86**, 368-375.
2. Y. Wang and L. Guo, *Mycosystema*, 2004, **23**, 474-479.
3. S. A. Mapari, A. S. Meyer and U. Thrane, *Biotechnology letters*, 2008, **30**, 2183-2190.
4. M. A. Larkin, G. Blackshields, N. Brown, R. Chenna, P. A. McGettigan, H. McWilliam, F. Valentin, I. M. Wallace, A. Wilm and R. Lopez, *bioinformatics*, 2007, **23**, 2947-2948.
5. N. Saitou and M. Nei, *Molecular biology and evolution*, 1987, **4**, 406-425.
6. S. Kumar, G. Stecher and K. Tamura, *Molecular biology and evolution*, 2016, **33**, 1870-1874.
7. J. T. Simpson, K. Wong, S. D. Jackman, J. E. Schein, S. J. Jones and I. Birol, *Genome research*, 2009, **19**, 1117-1123.
8. R. Li, Y. Li, K. Kristiansen and J. Wang, *Bioinformatics*, 2008, **24**, 713-714.
9. D. R. Zerbino and E. Birney, *Genome research*, 2008, **18**, 821-829.
10. M. B. Clamp and R. Durbin, *Genome Res.*, 2004, **14**, 988-995.
11. L. C. de Lima Favaro, F. L. de Melo, C. I. Aguilar-Vildoso and W. L. Araujo, *PloS one*, 2011, **6**.
12. J. Watrous, P. Roach, T. Alexandrov, B. S. Heath, J. Y. Yang, R. D. Kersten, M. van der Voort, K. Pogliano, H. Gross and J. M. Raaijmakers, *Proceedings of the National Academy of Sciences*, 2012, **109**, E1743-E1752.
13. Gaussian 03, Revision C.02, M. J. Frisch, G. W. Trucks, H. B. Schlegel, G. E. Scuseria, M. A. Robb, J. R. Cheeseman, J. A. Montgomery, Jr., T. Vreven, K. N. Kudin, J. C. Burant, J. M. Millam, S. S. Iyengar, J. Tomasi, V. Barone, B. Mennucci, M. Cossi, G. Scalmani, N. Rega, G. A. Petersson, H. Nakatsuji, M. Hada, M. Ehara, K. Toyota, R. Fukuda, J. Hasegawa, M. Ishida, T. Nakajima, Y. Honda, O. Kitao, H. Nakai, M. Klene, X. Li, J. E. Knox, H. P. Hratchian, J. B. Cross, V. Bakken, C. Adamo, J. Jaramillo, R. Gomperts, R. E. Stratmann, O. Yazyev, A. J. Austin, R. Cammi, C. Pomelli, J. W. Ochterski, P. Y. Ayala, K. Morokuma, G. A. Voth, P. Salvador, J. J. Dannenberg, V. G. Zakrzewski, S. Dapprich, A. D. Daniels, M. C. Strain, O. Farkas, D. K. Malick, A. D. Rabuck, K. Raghavachari, J. B. Foresman, J. V. Ortiz, Q. Cui, A. G. Baboul, S. Clifford, J. Cioslowski, B. B. Stefanov, G. Liu, A. Liashenko, P. Piskorz, I. Komaromi, R. L. Martin, D. J. Fox, T. Keith, M. A. Al-Laham, C. Y. Peng, A. Nanayakkara, M. Challacombe, P. M. W. Gill, B. Johnson, W. Chen, M. W. Wong, C. Gonzalez, and J. A. Pople, Gaussian, Inc., Wallingford CT, 2004.
14. Cammi, R.; Tomasi, J. *J. Comput. Chem.* 1995, **16**, 1449–1458.
15. Gross, E. K. U.; Dobson, J. F.; Petersilka, M. *Density Functional Theory II*. 1996, 81–172.

16. F. Song, X. Liu, H. Guo, B. Ren, C. Chen, A. M. Piggott, K. Yu, H. Gao, Q. Wang and M. Liu, *Organic letters*, 2012, **14**, 4770-4773.
17. A. W. Fothergill, in *Interactions of yeasts, moulds, and antifungal agents*, Springer, 2012, pp. 65-74.
18. K. Blin, T. Wolf, M. G. Chevrette, X. Lu, C. J. Schwalen, S. A. Kautsar, H. G. Suarez Duran, E. L. de Los Santos, H. U. Kim and M. Nave, *Nucleic acids research*, 2017, **45**, W36-W41.
19. A. Jacob, J. Lancaster, J. Buhler, B. Harris and R. D. Chamberlain, *ACM Transactions on Reconfigurable Technology and Systems (TRETS)*, 2008, **1**, 1-44.
20. I. Letunic and P. Bork, *Nucleic acids research*, 2011, **39**, W475-W478.
21. I. Letunic and P. Bork, *Bioinformatics*, 2006, **23**, 127-128.
22. N. L. Catlett, B.-N. Lee, O. Yoder and B. G. Turgeon, *Fungal Genetics Reports*, 2003, **50**, 9-11.
23. J. Liu, T. Hao, P. Hu, Y. Pan, X. Jiang and G. Liu, *Fungal Genetics and Biology*, 2017, **107**, 67-76.